BACHELOR

The spherical pendulum
different solutions on a 2-sphere

Dohmen, Jesse L.P.

Award date:
2017

The Spherical Pendulum:
Different Solutions on a 2-Sphere

Bachelor Final Project Applied Mathematics
Eindhoven University of Technology
Supervisor: J.C. van der Meer

by Jesse Dohmen 0899975

August 13, 2017

1 Introduction

A well-known problem from mathematical physics is the simple (mathematical) pendulum, in which the movement of a pendulum through a plane is described. The trajectory of the pendulum is along a circle.
By generalising this movement to a 3-dimensional space, we obtain the spherical pendulum. An example of a spherical pendulum is Foucalt's pendulum, which is a big pendulum that is aimed to demonstrate the rotation of the Earth. These pendulums are located in various museums and universities, like the Radboud University in Nijmegen. The spherical pendulum is the research topic of this project.

1.1 Physical situation

The physical situation is as follows. The suspension point of the pendulum is located in the centre of a 2-sphere with radius 1. A ***2-sphere*** S^2 is the set of all points equidistant to a central point in $\mathbb{R}^3$. In other words, it is the surface of a sphere in a 3-dimensional space like $\mathbb{R}^3$. The other endpoint of the pendulum is a mass concentrated in one point that moves on the 2-sphere. There is also only one gravitational force acting on the endpoint of the pendulum, and no friction is involved in this problem. The connection between the endpoints is a rigid massless rope.

1.2 Coordinate spaces

Let q and p denote the ***canonical coordinates*** of the physical system, with q the coordinate vector on the 2-sphere and p the momentum vector tangent to the 2-sphere at point q. So the momenta p are perpendicular to the coordinates q. These are coordinates that can be used to describe a physical system at any given point in time. The 3 coordinates q_1, q_2, q_3 are in the so called ***configuration space***, which is the vector space defined by the coordinate vectors q. Tangent to points q on the 2-sphere S^2 are tangent planes spanned by the momenta p. All these planes together with the points they are tangent to form the ***tangent bundle*** TS^2. The tangent bundle is the phase space of this problem. A ***phase space*** is a space in which all possible states of a dynamical system are represented, with each point in the phase space representing a state of the system at a certain time t. The system which will be investigated can be described by a Hamiltonian system, which is a well known system when it comes to classic mechanical problems like the spherical pendulum.

1.3 Overview

Let us now give an overview of the project.
The so called Poisson-brackets are introduced in the next section. This will be the main tool used in this report to describe Hamiltonian systems.
As an introduction to the details of the spherical pendulum, section 3 deals with the mathematical pendulum. This section is aimed to give the reader a feel of what is coming next in the report.
In section 4 the Hamiltonian equations for the spherical pendulum are being stated.
Section 5 deals with integrals that will help to characterise periodic solutions of the Hamilton equations. Also Liouville's Integrability theorem will be introduced, which plays a central role in the theory of Hamiltonian dynamics.
Furthermore, in section 6 the Energy-Momentum-Mapping together with his critical values is considered, which is a begin to the depicting of the phase space and the configuration space (the real movement of the pendulum).
In section 7 the classification of the solutions that belong to the critical values of the Energy-Momentum-Mapping is treated. The movements of the pendulum that are determined by these solutions will also be illustrated.

2 Poisson-brackets

In this section the so called Poisson-brackets are introduced. Poisson-brackets are an important tool in the study of Hamiltonian equations. Although it is named after the Siméon Denis Poisson, he was not the one who was mainly busy with it.

2.1 Definition of Poisson-bracket

Let q_i and p_i with $i \in \{1, ..., N\}$ be the coordinates of the vector (q, p) in the $2N$-dimensional space M and let $f \in C^\infty(M)$ and $g \in C^\infty(M)$, where $C^\infty(M)$ denotes the space of all infinitely continuously differentiable functions that take elements of the space M and map it to $\mathbb{R}$. Then the Poisson-bracket is defined as the following.

Definition 2.1 (Poisson-bracket) *A bracket is a **Poisson-bracket** if it is a map* $\{\cdot,\cdot\} : C^\infty(M)\times C^\infty(M) \to C^\infty(M)$*, which satisfies the next 4 properties:*

- *Anticommutativity:* $\{f, g\} = -\{g, f\}$.
- *Distributivity:* $\{f + g, h\} = \{f, h\} + \{g, h\}$.
- *Product rule (Also known as Leibniz-identity):* $\{fg, h\} = g\{f, h\} + f\{g, h\}$.
- *Jacobi-identity:* $\{f, \{g, h\}\} + \{g, \{h, f\}\} + \{h, \{f, g\}\} = 0$.

There is one form of a Poisson-bracket that is interesting for us to investigate, namely the so called Standard Poisson-bracket.

Definition 2.2 (Standard Poisson-bracket) *The **Standard Poisson-bracket*** $\{f, g\}$ *for functions* $f \in C^\infty(M)$ *and* $g \in C^\infty(M)$*, is defined as*

$$\{f, g\} = \sum_{i=1}^{N} \Big(\frac{\partial f}{\partial q_i}\frac{\partial g}{\partial p_i} - \frac{\partial f}{\partial p_i}\frac{\partial g}{\partial q_i}\Big) .$$

The claim is now that the Standard Poisson-bracket suffices the properties of a Poisson-bracket. So to proof this, these properties need to be checked.

Theorem 2.3 *The Standard Poisson-bracket is a Poisson-bracket.*

Proof:

- Anticommutativity:

$$\{f, g\} = \sum_{i=1}^{N} \Big(\frac{\partial f}{\partial q_i}\frac{\partial g}{\partial p_i} - \frac{\partial f}{\partial p_i}\frac{\partial g}{\partial q_i}\Big) = -\sum_{i=1}^{N} \Big(\frac{\partial f}{\partial p_i}\frac{\partial g}{\partial q_i} - \frac{\partial f}{\partial q_i}\frac{\partial g}{\partial p_i}\Big) = -\{g, f\} .$$

- Distributivity:

$$\begin{aligned}
\{f + g, h\} &= \sum_{i=1}^{N} \Big(\frac{\partial (f+g)}{\partial q_i}\frac{\partial h}{\partial p_i} - \frac{\partial (f+g)}{\partial p_i}\frac{\partial h}{\partial q_i}\Big) ,\\
&= \sum_{i=1}^{N} \Big(\frac{\partial f}{\partial q_i}\frac{\partial h}{\partial p_i} - \frac{\partial f}{\partial p_i}\frac{\partial h}{\partial q_i} + \frac{\partial g}{\partial q_i}\frac{\partial h}{\partial p_i} - \frac{\partial g}{\partial p_i}\frac{\partial h}{\partial q_i}\Big) ,\\
&= \sum_{i=1}^{N} \Big(\frac{\partial f}{\partial q_i}\frac{\partial h}{\partial p_i} - \frac{\partial f}{\partial p_i}\frac{\partial h}{\partial q_i}\Big) + \sum_{i=1}^{N} \Big(\frac{\partial g}{\partial q_i}\frac{\partial h}{\partial p_i} - \frac{\partial g}{\partial p_i}\frac{\partial h}{\partial q_i}\Big) ,\\
&= \{f, h\} + \{g, h\} .
\end{aligned}$$

- Product rule (Leibniz rule):

$$
\begin{aligned}
\{fg,h\} &= \sum_{i=1}^{N}\Big(\frac{\partial fg}{\partial q_i}\frac{\partial h}{\partial p_i} - \frac{\partial fg}{\partial p_i}\frac{\partial h}{\partial q_i}\Big)\ , \\
&= \sum_{i=1}^{N}\Big(\Big(f\frac{\partial g}{\partial q_i} + g\frac{\partial f}{\partial q_i}\Big)\frac{\partial h}{\partial p_i} - \Big(f\frac{\partial g}{\partial p_i} + g\frac{\partial f}{\partial p_i}\Big)\frac{\partial h}{\partial q_i}\Big)\ , \\
&= \sum_{i=1}^{N} f\Big(\frac{\partial g}{\partial q_i}\frac{\partial h}{\partial p_i} - \frac{\partial g}{\partial p_i}\frac{\partial h}{\partial q_i}\Big) + \sum_{i=1}^{N} g\Big(\frac{\partial f}{\partial q_i}\frac{\partial h}{\partial p_i} - \frac{\partial f}{\partial p_i}\frac{\partial h}{\partial q_i}\Big)\ , \\
&= f\sum_{i=1}^{N}\Big(\frac{\partial g}{\partial q_i}\frac{\partial h}{\partial p_i} - \frac{\partial g}{\partial p_i}\frac{\partial h}{\partial q_i}\Big) + g\sum_{i=1}^{N}\Big(\frac{\partial f}{\partial q_i}\frac{\partial h}{\partial p_i} - \frac{\partial f}{\partial p_i}\frac{\partial h}{\partial q_i}\Big)\ , \\
&= f\{g,h\} + g\{f,h\}\ .
\end{aligned}
$$

- Jacobi-identity: Let f and g and h be functions of some $a \in \{q_1, ..., q_N, p_1, ..., p_N\}$. The the next identity holds,

$$
\begin{aligned}
\frac{\partial}{\partial a}\{f,g\} &= \frac{\partial}{\partial a}\sum_{i=1}^{N}\Big(\frac{\partial f}{\partial q_i}\frac{\partial g}{\partial p_i} - \frac{\partial f}{\partial p_i}\frac{\partial g}{\partial q_i}\Big)\ , \\
&= \sum_{i=1}^{N}\Big(\frac{\partial^2 f}{\partial a\partial q_i}\frac{\partial g}{\partial p_i} - \frac{\partial^2 f}{\partial a\partial p_i}\frac{\partial g}{\partial q_i} + \frac{\partial f}{\partial q_i}\frac{\partial^2 g}{\partial a\partial p_i} - \frac{\partial f}{\partial p_i}\frac{\partial^2 g}{\partial a\partial q_i}\Big)\ , \\
&= \{\frac{\partial f}{\partial a}, g\} + \{f, \frac{\partial g}{\partial a}\}\ .
\end{aligned}
$$

Now the Poisson-bracket $\{h,\{f,g\}\}$ can be expanded as follows,

$$\begin{aligned}
\{h,\{f,g\}\} &= \Big\{h,\sum_{i=1}^{N}\Big(\frac{\partial f}{\partial q_i}\frac{\partial g}{\partial p_i}-\frac{\partial f}{\partial p_i}\frac{\partial g}{\partial q_i}\Big)\Big\} \ ,\\
&= \sum_{i=1}^{N}\Big(\Big\{h,\frac{\partial f}{\partial q_i}\frac{\partial g}{\partial p_i}\Big\}-\Big\{h,\frac{\partial f}{\partial p_i}\frac{\partial g}{\partial q_i}\Big\}\Big) \text{ (by the distributivity property) },\\
&= \sum_{i=1}^{N}\Big(\frac{\partial f}{\partial q_i}\Big\{h,\frac{\partial g}{\partial p_i}\Big\}+\frac{\partial g}{\partial p_i}\Big\{h,\frac{\partial f}{\partial q_i}\Big\}-\frac{\partial f}{\partial p_i}\Big\{h,\frac{\partial g}{\partial q_i}\Big\}-\frac{\partial g}{\partial q_i}\Big\{h,\frac{\partial f}{\partial p_i}\Big\}\Big) \text{ (by the product rule) },\\
&= \sum_{i=1}^{N}\Big(\frac{\partial f}{\partial q_i}\Big(\frac{\partial}{\partial p_i}\{h,g\}-\Big\{\frac{\partial h}{\partial p_i},g\Big\}\Big)+\frac{\partial g}{\partial p_i}\Big(\frac{\partial}{\partial q_i}\{h,f\}-\Big\{\frac{\partial h}{\partial q_i},f\Big\}\Big)\\
&\quad -\frac{\partial f}{\partial p_i}\Big(\frac{\partial}{\partial q_i}\{h,g\}-\Big\{\frac{\partial h}{\partial q_i},g\Big\}\Big)-\frac{\partial g}{\partial q_i}\Big(\frac{\partial}{\partial p_i}\{h,f\}-\Big\{\frac{\partial h}{\partial p_i},f\Big\}\Big)\Big) \text{ (by the earlier established identity) },\\
&= -\{f,\{g,h\}\}-\{g,\{h,f\}\}+\sum_{i=1}^{N}\Big(-\frac{\partial f}{\partial q_i}\Big\{\frac{\partial h}{\partial p_i},g\Big\}-\frac{\partial g}{\partial p_i}\Big\{\frac{\partial h}{\partial q_i},f\Big\}+\frac{\partial f}{\partial p_i}\Big\{\frac{\partial h}{\partial q_i},g\Big\}+\frac{\partial g}{\partial q_i}\Big\{\frac{\partial h}{\partial p_i},f\Big\}\Big) \ ,\\
&= -\{f,\{g,h\}\}-\{g,\{h,f\}\}+\sum_{i,j=1}^{N}\frac{\partial f}{\partial q_i}\frac{\partial^2 h}{\partial p_i\partial q_j}\frac{\partial g}{\partial p_j}+\sum_{i,j=1}^{N}\frac{\partial f}{\partial q_i}\frac{\partial^2 h}{\partial p_i\partial p_j}\frac{\partial g}{\partial q_j}\\
&\quad -\sum_{i,j=1}^{N}\frac{\partial g}{\partial p_i}\frac{\partial^2 h}{\partial q_i\partial q_j}\frac{\partial f}{\partial p_j}+\sum_{i,j=1}^{N}\frac{\partial g}{\partial p_i}\frac{\partial^2 h}{\partial q_i\partial p_j}\frac{\partial f}{\partial q_j}\\
&\quad +\sum_{i,j=1}^{N}\frac{\partial f}{\partial p_i}\frac{\partial^2 h}{\partial q_i\partial q_j}\frac{\partial g}{\partial p_j}-\sum_{i,j=1}^{N}\frac{\partial f}{\partial p_i}\frac{\partial^2 h}{\partial q_i\partial p_j}\frac{\partial g}{\partial q_j}\\
&\quad +\sum_{i,j=1}^{N}\frac{\partial g}{\partial q_i}\frac{\partial^2 h}{\partial p_i\partial q_j}\frac{\partial f}{\partial p_j}-\sum_{i,j=1}^{N}\frac{\partial g}{\partial q_i}\frac{\partial^2 h}{\partial p_i\partial p_j}\frac{\partial f}{\partial q_j} \ .
\end{aligned}$$

Since each term is summed over all i and j, each term is symmetric in i and j. So all pairs of terms where q_i and q_j are replaced by p_i and p_j respectively cancel out and what remains is

$$\{h,\{f,g\}\} = -\{f,\{g,h\}\}-\{g,\{h,f\}\} \ .$$

Bringing the right-hand side to the left gives the Jacobi-identity. [1]

2.2 Some important identities

There are some interesting identities that follow when taking the Poisson-Bracket of the coordinates q and p.

- $\{q_i,q_j\} = \sum_{k=1}^{N}\Big(\frac{\partial q_i}{\partial q_k}\frac{\partial q_j}{\partial p_k}-\frac{\partial q_i}{\partial p_k}\frac{\partial q_j}{\partial q_k}\Big) = 0$.

  Likewise it is true that $\{p_i,p_j\} = 0$.

- $\{q_i,p_j\} = \sum_{k=1}^{N}\Big(\frac{\partial q_i}{\partial q_k}\frac{\partial p_j}{\partial p_k}-\frac{\partial q_i}{\partial p_k}\frac{\partial p_j}{\partial q_k}\Big) = \sum_{k=1}^{N}\frac{\partial q_i}{\partial q_k}\frac{\partial p_j}{\partial p_k} = \frac{\partial p_j}{\partial p_i} = \delta_{ij}$, where $\delta_{ij} = \begin{cases}1 & \text{if i = j}\\ 0 & \text{else}\end{cases}$.

  Using the Anti-symmetry property it follows that $\{p_j,q_i\} = -\{q_i,p_j\} = -\delta_{ij}$.
  These equalities hold because only $\partial q_i/\partial q_i$ and $\partial p_i/\partial p_i$ are not zero. This follows from the fact that q_i and p_i are the independent coordinates for the space $\mathbb{R}^{2N}$.

Let $\mathbb{J} = \begin{pmatrix} (\{q_i, q_j\}) & (\{q_i, p_j\}) \\ (\{p_i, q_j\}) & (\{p_i, p_j\}) \end{pmatrix}$, with $(\{\cdot, \cdot\})$ an N-dimensional matrix of standard Poisson-brackets.
The identities $\{q_i, q_j\} = 0$, $\{p_i, p_j\} = 0$, $\{q_i, p_j\} = \delta_{ij}$ and $\{p_i, q_j\} = -\delta_{ij}$ imply that $\mathbb{J}$ looks like the following, with $N = 3$ as an example,

$$\mathbb{J} = \begin{pmatrix} 0 & 0 & 0 & 1 & 0 & 0 \\ 0 & 0 & 0 & 0 & 1 & 0 \\ 0 & 0 & 0 & 0 & 0 & 1 \\ -1 & 0 & 0 & 0 & 0 & 0 \\ 0 & -1 & 0 & 0 & 0 & 0 \\ 0 & 0 & -1 & 0 & 0 & 0 \end{pmatrix} .$$

With this matrix the standard Poisson bracket of arbitrary functions $f \in C^\infty(M)$ and $g \in C^\infty(M)$ can be expressed in the next way,

$$\{f, g\} = (\nabla f)^T \mathbb{J} \nabla g \ .$$

- $\{q_i, H\} = \sum_{k=1}^{N} \left(\frac{\partial q_i}{\partial q_k} \frac{\partial H}{\partial p_k} - \frac{\partial q_i}{\partial p_k} \frac{\partial H}{\partial q_k} \right) = \frac{\partial H}{\partial p_i}.$

  The function H can be regarded as the Hamiltonian, which will be explained later on.
  The latter holds because
  $$\frac{\partial q_i}{\partial q_k} = \begin{cases} 0 & \text{if } k \neq i \\ 1 & \text{if } k = i \end{cases}$$
  and
  $$\frac{\partial q_i}{\partial p_k} = 0 \ \forall k \in \{1, ..., N\}$$
  In the same way it can be computed that $\{p_i, H\} = -\partial H / \partial q_i$.
  From this it follows immediately that
  $$\{(q, p), H\} = \begin{pmatrix} \partial H/\partial p_1 \\ \partial H/\partial p_2 \\ \partial H/\partial p_3 \\ -\partial H/\partial q_1 \\ -\partial H/\partial q_2 \\ -\partial H/\partial q_3 \end{pmatrix} = \mathbb{J} \nabla H \ .$$

3 Mathematical Pendulum

Before we are getting into the details about the spherical pendulum it is handy to talk about the mathematical pendulum, which is a pendulum through a plane.
In this case, the suspension point of the pendulum is located in the midpoint of a circle with radius 1. The other endpoint of the pendulum is located on the circle.
The goal is to find the function known as the Hamiltonian. The Hamiltonian is a function that describes the total energy of a physical system. It is a function of the canonical coordinates q and p. First the law of conservation of energy will be applied to find the Hamiltonian H of a free moving particle under the influence of gravity. Here the coordinates (q, p) are coordinates in the 4-dimensional space $T\mathbb{R}^2$, which consists of all pairs (q, p) in $\mathbb{R}^4$ for which p is tangent to q. Then the Hamiltonian H^* for the mathematical pendulum will be found by constraining the first found Hamiltonian H to the circle. And so the coordinates (q, p) are part of the tangent bundle TS^1.

3.1 Hamiltonian in $T\mathbb{R}^2$

Let $q \in \mathbb{R}^2$ be the position in m, $t \in \mathbb{R}$ the time in s and $p = m\dot{q} = m(dq/dt)$ the momentum in kg $\cdot$ (m/s), with m the mass of the endpoint of the pendulum.
Furthermore, let E_{tot} be the total energy, E_{kin} the kinetic energy and E_{pot} the potential energy in J.
In this case, E_{pot} is just the gravitational energy.
The Hamiltonian of a free moving particle under the influence of gravity can be found using the law of conservation of energy,

$$E_{\text{tot}} = E_{\text{kin}} + E_{\text{pot}} \ .$$

Now $E_{\text{kin}} = \dfrac{p_1^2 + p_2^2}{2m}$ and $E_{\text{pot}} = -mgq_2$, so

$$H(p, q) = E_{\text{tot}} = \frac{p_1^2 + p_2^2}{2m} - mgq_2 \ . \tag{1}$$

It is important to note that the Hamiltonian is not explicitly dependent on the time t, which makes it invariant and constant along solutions. More of this will be explained later on in section 5.
There is a system of four Hamiltonian equations that follows from this,

$$\begin{aligned}
\frac{p_1}{dt} &= -\frac{\partial H}{\partial q_1} = 0 \ , \\
\frac{p_2}{dt} &= -\frac{\partial H}{\partial q_2} = mg \ , \\
\frac{q_1}{dt} &= -\frac{\partial H}{\partial p_1} = \frac{p_1}{m} \ , \\
\frac{q_2}{dt} &= -\frac{\partial H}{\partial p_2} = \frac{p_2}{m} \ .
\end{aligned}$$

A change of coordinates has to be chosen to make the problem dimensionless. This makes it more convenient to work with the coordinates.
To find such a change, let $p_i = c_1 y_i$ and let $q_i = c_2 x_i$ $\forall i \in \{1, 2\}$. Substituting this in the Hamiltonian system gives $c_1 = mg$ and $c_2 = g$. So if we choose $p = mgy$ and $q = gx$, then the

system changes to

$$\frac{dy_1}{dt} = -\frac{\partial H}{\partial q_1} = 0 \ ,$$
$$\frac{dy_2}{dt} = -\frac{\partial H}{\partial q_2} = 0 \ ,$$
$$\frac{dx_1}{dt} = \frac{\partial H}{\partial p_1} = y_1 \ ,$$
$$\frac{dx_2}{dt} = \frac{\partial H}{\partial p_2} = y_2 \ .$$

3.2 Hamiltonian in TS^1

The space $T\mathbb{R}^2$ concerns all points in $\mathbb{R}^2$, but we have to keep in mind that the pendulum only moves on a circle and not on the whole $\mathbb{R}^2$.
This means that the position x of the pendulum is constrained to

$$||x||^2 = x_1^2 + x_2^2 = 1 \ .$$

Here $||\cdot||$ denotes the vector two-norm. This holds if the radius of the circle is equal to one and the origin of the coordinate plane is located at the centre of the circle.
The momentum y is also constrained to a certain condition. Because y has to be tangent to the circle at point x, it has to be orthogonal to the coordinate vector x. Let $< \ , \ >$ denote the inner product of two vectors. So we have

$$< x, y >= x_1 y_1 + x_2 y_2 = 0 \ .$$

Hence the phase space has been reduced from a four-dimensional space $T\mathbb{R}^2$ to a two-dimensional tangent bundle TS^1 due to these two constraints.
As a consequence of this conversion it is not convenient anymore to work with the Hamiltonian H, but another Hamiltonian H^* is needed that takes the two constraints into account. This H^* is chosen in such a way that the constraints $||x|| = 1$ and $< x, y >= 0$ are incorporated in the definition of H^*. As a result of that, the terms of H^* that are multiples of expressions that vanish on points on the circle cancel out. It turns out that at these points H^* is still a Hamiltonian. For more details, see [2]. Let e_i be the standard basis vector, so $e_i = (0, 0, ..., 1, 0, ..., 0)$ with a 1 on the i-th spot. Then the constrained Hamiltonian H^* can be written as

$$H^*(x, y) = \frac{1}{2} < y, y > + < x, e_2 > + \frac{1}{2}(< y, y > - < x, e_2 >)(< x, x > -1) - \frac{1}{2} < x, y >^2 \ .$$

Let $X_{H^*}(x, y) = (dx/dt, dy/dt) = \begin{pmatrix} \partial H^*/\partial y \\ -\partial H^*/\partial x \end{pmatrix}$ be the Hamiltonian vector field of the constrained Hamiltonian H^*. Calculating $\partial H^*/\partial y$ and $-\partial H^*/\partial x$ then yields

$$\begin{aligned} \frac{dx}{dt} &= y + y(< x, x > -1) - < x, y > x \ , \\ \frac{dy}{dt} &= -e_2 + \frac{1}{2} e_2(< x, x > -1) - (< y, y > - < x, e_2 >)x + < x, y > y \ . \end{aligned} \tag{2}$$

It is true that the components of X_{H^*} are tangent to the tangent bundle TS^1 and that they form the flow on the tangent bundle of the constrained Hamiltonian. More on the flow will be explained later on in section 5. Using the identities $< x, x >= 1$ and $< x, y >= 0$, equations (2) reduce to

$$\dot{x} = y \ ,$$
$$\dot{y} = -e_2 + (< x, e_2 > - < y, y >)x \ .$$

In Figure 1 the circle with the pendulum (red) can be seen. The momentum p, tangent to the circle, together with the red point q span the tangent bundle TS^1.

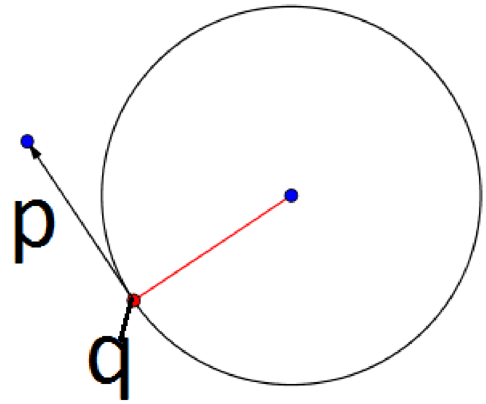

Figure 1: The situation for the mathematical pendulum

3.3 Energy mapping

As we know, the constrained Hamiltonian H^* is a function that describes the total energy in a system. It is thus interesting to consider a mapping that translates this energy from the tangent bundle to the constrained Hamiltonian. This mapping is called the Energy mapping and is given by

$$E : TS^1 \subseteq T\mathbb{R}^2 \to \mathbb{R} :$$
$$(x, y) \to H^* = \frac{1}{2}(y_1^2 + y_2^2) + x_2 \ .$$

The image consists only of the constrained Hamiltonian H^*. The critical values of this Energy mapping are then those values for x and y for which $\nabla H^* = 0$, or for which $\dot{x}$ and $\dot{y}$ are equal to zero. These solutions are then called stationary solutions and they are found by solving

$$\dot{x} = y = 0 \ ,$$
$$\dot{y} = -e_2 + (< x, e_2 > - < y, y >)x = 0 \ .$$

From this it immediately follows that $x_1 = 0$, $x_2 = \pm 1$, $y_1 = 0$ and $y_2 = 0$. The stationary solutions are thus $(0, \pm 1, 0, 0)$ in the phase space. So the critical values of the Energy-Mapping are $H^* = \frac{1}{2}(y_1^2 + y_2^2) + x_2 = \pm 1$. As $\frac{1}{2}(y_1^2 + y_2^2) \geq 0$ and $-1 \leq x_2 \leq 1$ it is also immediately clear that $H^* \geq -1$.
Now we turn to the classification of the solutions.

- If $H = -1$, then the pendulum rests in the point $(0, -1, 0, 0)$. This is a stable solution.
- If $H = 1$, then the pendulum rests in the point $(0, 1, 0, 0)$. This is an unstable solution.
- If $H^* \notin \{-1, 1\}, H^* > -1$, then the pendulum swings on the circle. The value of H^* determines the highest value of x_2 the pendulum reaches.

4 Hamiltonian equations

The goal of this section is to find the Hamiltonian in the case of the spherical pendulum. First the law of conservation of energy will be applied to find the Hamiltonian H of a free moving particle under the influence of gravity. Here the coordinates (q,p) are coordinates in the 6-dimensional space $T\mathbb{R}^3$, which consists of all pairs (q,p) in $\mathbb{R}^6$ for which p is tangent to q. Then the Hamiltonian H^* for the mathematical pendulum will be found by constraining the first found Hamiltonian H to the circle. And so the coordinates (q,p) are part of the tangent bundle TS^2.

4.1 Hamiltonian in $T\mathbb{R}^3$

Again, let $q \in \mathbb{R}^3$ be the position in m, $t \in \mathbb{R}$ the time in q and $p = m\dot{q} = m\dfrac{dq}{dt}$ the velocity in kg $\cdot$ (m/s).
Furthermore, let E_{tot} be the total energy, E_{kin} the kinetic energy and E_{pot} the potential energy in J.
Now the Hamiltonian can be found using the law of conservation of energy

$$E_{\text{tot}} = E_{\text{kin}} + E_{\text{pot}} \ .$$

Now $E_{\text{kin}} = \dfrac{p_1^2 + p_2^2 + p_3^2}{2m}$ and $E_{\text{pot}} = -mgq_3$, so

$$H(p,q) = E_{\text{tot}} = \frac{p_1^2 + p_2^2 + p_3^2}{2m} - mgq_3 \ . \tag{3}$$

There is a system of six Hamiltonian equations that follows from this,

$$\begin{aligned}
\frac{dp_1}{dt} &= -\frac{\partial H}{\partial q_1} = 0 \ , \\
\frac{dp_2}{dt} &= -\frac{\partial H}{\partial q_2} = 0 \ , \\
\frac{dp_3}{dt} &= -\frac{\partial H}{\partial q_3} = mg \ , \\
\frac{dq_1}{dt} &= \frac{\partial H}{\partial p_1} = \frac{p_1}{m} \ , \\
\frac{dq_2}{dt} &= \frac{\partial H}{\partial p_2} = \frac{p_2}{m} \ , \\
\frac{dq_3}{dt} &= \frac{\partial H}{\partial p_3} = \frac{p_3}{m} \ .
\end{aligned}$$

In section 1 a change of coordinates was found to make the problem dimensionless. The results were $q = gx$ and $p = mgy$. The system of equations then changes to

$$\begin{aligned}
\frac{dy_1}{dt} &= -\frac{\partial H}{\partial q_1} = 0, \\
\frac{dy_2}{dt} &= -\frac{\partial H}{\partial q_2} = 0, \\
\frac{dy_3}{dt} &= -\frac{\partial H}{\partial q_3} = 1, \\
\frac{dx_1}{dt} &= \frac{\partial H}{\partial p_1} = y_1, \\
\frac{dx_2}{dt} &= \frac{\partial H}{\partial p_2} = y_2, \\
\frac{dx_3}{dt} &= \frac{\partial H}{\partial p_3} = y_3 \ .
\end{aligned}$$

One can describe a Hamiltonian system in terms of Poisson-brackets in the following way, with $z \in C^\infty(T\mathbb{R}^3)$ an arbitrary function that is not explicitly dependent on the time t,

$$\dot{z} = \{z, H\} \ .$$

This identity follows by the next reasoning.

$$\dot{z} = \frac{dz}{dt} = \sum_{i=1}^{3} \frac{\partial z}{\partial x_i}\frac{dx_i}{dt} + \sum_{i=1}^{3} \frac{\partial z}{\partial y_i}\frac{dy_i}{dt} \ .$$

This is the directional derivative of z to the components of the basis vectors that span $T\mathbb{R}^3$.
Now substitute the Hamiltonian equations $dx_i/dt = \partial H/\partial y_i$ and $dy_i/dt = -\partial H/\partial x_i$ for $\dot{x}$ and $\dot{y}$ to get

$$\dot{z} = (\nabla z)^T \begin{pmatrix} \partial H/\partial y_1 \\ \partial H/\partial y_2 \\ \partial H/\partial y_3 \\ -\partial H/\partial x_1 \\ -\partial H/\partial x_2 \\ -\partial H/\partial x_3 \end{pmatrix} \ .$$

The second remark in section 2 says that this is equal to

$$\dot{z} = (\nabla z)^T \mathbb{J} \nabla H = \{z, H\} \ .$$

Likewise, for the position and momentum variables x and y the next holds,

$$\begin{pmatrix} \dot{x} \\ \dot{y} \end{pmatrix} = \{(x, y)^T, H\} = \mathbb{J}\nabla H = \begin{pmatrix} \partial H/\partial y \\ -\partial H/\partial x \end{pmatrix} \ .$$

4.2 Hamiltonian in TS^2

The space $T\mathbb{R}^3$ concerns all points in $\mathbb{R}^3$, but we have to keep in mind that the pendulum only moves on a two-sphere and not on the whole $\mathbb{R}^3$.
So the position x of the pendulum is constrained to

$$||x||^2 = x_1^2 + x_2^2 + x_3^2 = 1 \ .$$

This holds if the radius of the sphere is equal to one and the origin of the coordinate plane is located at the centre of the sphere.
The momentum y is also constrained in the way that it has to be orthogonal to a certain point on the manifold, because it has to be tangent to the sphere, so

$$< x, y >= x_1 y_1 + x_2 y_2 + x_3 y_3 = 0 \ .$$

If this was not the case, then the pendulum would have the intention to go away from the two-sphere, which is an undesirable property.
So the phase space has been reduced from a 6-dimensional space $T\mathbb{R}^3$ to a four-dimensional tangent bundle TS^2 due to these two constraints.
Due to this conversion it is not convenient anymore to work with the Hamiltonian H, but another Hamiltonian H^* is needed that takes the two constraints into account. This H^* is chosen in such a way that the constraints $||x|| = 1$ and $< x, y >= 0$ are incorporated in the definition of H^*. As a result of that, the terms of H^* that are multiples of expressions that vanish on points on the circle cancel out. It turns out that at these points H^* is still a Hamiltonian. For more details, see [2].

$$H^*(x, y) = \frac{1}{2} < y, y > + < x, e_3 > + \frac{1}{2}(< y, y > - < x, e_3 >)(< x, x > -1) - \frac{1}{2} < x, y >^2 \ .$$

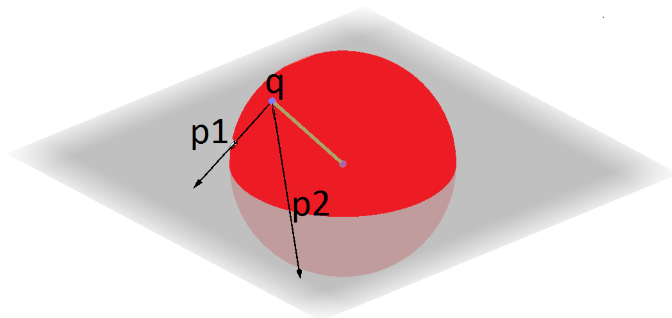

Figure 2: The situation for the spherical pendulum

Let $X_{H^*}(x,y) = (dx/dt, dy/dt) = \begin{pmatrix} \partial H^*/\partial y \\ -\partial H^*/\partial x \end{pmatrix}$ be the Hamiltonian vector field of the constrained Hamiltonian H^*. Calculating $\partial H^*/\partial y$ and $-\partial H^*/\partial x$ then yields

$$\begin{aligned} \frac{dx}{dt} &= y + y(< x, x > -1) - < x, y > x \ , \\ \frac{dy}{dt} &= -e_3 + \frac{1}{2} e_3(< x, x > -1) - (< y, y > - < x, e_3 >)x + < x, y > y \ . \end{aligned} \tag{4}$$

It is true that the components of X_{H^*} are tangent to the tangent bundle TS^2 and that they form the flow on the tangent bundle of the constrained Hamiltonian. More on the flow will be explained later on in section 5. Using the constraints $< x, x >= 1$ and $< x, y >= 0$, equations (4) reduce to

$$\begin{aligned} \dot{x} &= y \ , \\ \dot{y} &= -e_3 + (< x, e_3 > - < y, y >)x \ . \end{aligned}$$

In Figure 2 the sphere with pendulum (green) can be seen. The vectors $p1$ and $p2$ span the tangent plane tangent to the sphere at point q. Together with point q the plane forms the tangent bundle TS^2.

5 Integrability

5.1 Liouville's Integrability Theorem

In this section an important theorem is stated, known as Liouville's Integrability theorem. With this we can assign meaning to certain solutions of the Hamiltonian system of equations. But first we need to know what integrability means. In the broadest sense we mean with Integrability the finding of solutions $x(t)$ and $y(t)$ of the system

$$\begin{pmatrix} \dot{x} \\ \dot{y} \end{pmatrix} = X_H(x, y) \ .$$

for a general initial condition $x(t_0) = x_0$ and $y(t_0) = y_0$.
A helpful tool to find our periodic solutions is to find so called integrals that will characterise the solution. But what are integrals?

Definition 5.1 *A quantity A is an **integral** of a (Hamiltonian) vector field if it does not depend explicitly on the time t and is constant along solutions. Furthermore, the derivative of an integral in the direction of the vector field identically equals zero. Or, in terms of the Poisson-bracket,*

$$\{A, H\} = (\nabla A)^T \mathbb{J} \nabla H = 0 \ .$$

It is the case here that H denotes the Hamiltonian of the system.
The main theorem tells us that n integrals are enough to fully characterise a periodic solution in $2n$ equations, but before we introduce that, we first need to know what a diffeomorphism is.

Definition 5.2 *A **diffeomorphism** is a differentiable isomorphism of smooth spaces. An isomorphism is a bijective mapping that preserves algebraic structures, like vector spaces.*

Now the main theorem will be stated.

Theorem 5.3 (Liouville's Integrability Theorem) *Let H be the Hamiltonian of the system. A Hamiltonian system with n degrees of freedom is **Liouville integrable** if it has a set of n integrals F_i that are almost everywhere independent of each other, except on sets of Lebesgue-measure zero, if $\{F_i, H\} = 0 \ \forall i \in \{1, ..., n\}$ and if $\{F_i, F_j\} = 0 \ \forall i, j \in \{1, ..., n\}$, with F_i and F_j integrals of X_{H^*}.*
If this is the case, then if the level sets $L_{c_i} = \{F_i(p, q) = c_i\}$ are compact, they are diffeomorphic to n-dimensional invariant tori T^n.[3]

5.2 Integrals in the case of the Spherical Pendulum

There are 2 candidates to suffice the conditions for being integrals that satisfy the conditions for Liouville's Integrability Theorem. This is because the restriction to the tangent bundle of the 2-sphere is $2n = 4$-dimensional, with $n = 2$. The candidate quantities are the Hamiltonian $H^* = \frac{1}{2}(y_1^2 + y_2^2 + y_3^2) + x_3$ itself and the quantity $J = x_1 y_2 - x_2 y_1$. The flow on the Hamiltonian vector field of H^* describes the overall movement of the pendulum adding swinging. The flow on the Hamiltonian vector field of J describes the rotation around the x_3-axis. One can recognise J also as the third component of the vector product of x and y. So according to Liouville's Integrability Theorem they have to satisfy

$$\{H^*, J\} = 0 \ , \{H^*, H^*\} = 0 \ ,$$

in order to let their level sets be diffeomorphic to invariant 2-dimensional tori. To prove the claim that $\{H^*, J\} = 0$, we can write

$$\begin{aligned}
\{H^*, J\} &= \{H^*, x_1 y_2 - x_2 y_1\} \ , \\
&= -\{x_1 y_2 - x_2 y_1, H^*\} \ , \ \text{(by Anti} - \text{symmetry)} \\
&= -\Big(\{x_1 y_2, H^*\} - \{x_2 y_1, H^*\}\Big) \ , \ \text{(by distributivity)} \\
&= \{x_2 y_1, H^*\} - \{x_1 y_2, H^*\} \ , \\
&= x_2\{y_1, H^*\} + y_1\{x_2, H^*\} - x_1\{y_2, H^*\} - y_2\{x_1, H^*\} \ , \ \text{(by the product rule)} \\
&= -x_2 \frac{\partial H^*}{\partial x_1} + y_1 \frac{\partial H^*}{\partial y_2} + x_1 \frac{\partial H^*}{\partial x_2} - y_2 \frac{\partial H^*}{\partial y_1} \ , \ \text{(by the last remark in section 2)} \\
&= 0 + y_1 y_2 + 0 - y_1 y_2 = 0 \ .
\end{aligned}$$

The identity $\{H^*, H^*\} = 0$ can easily be confirmed by

$$\{H^*, H^*\} = (\nabla H^*)^T \mathbb{J} \nabla H = \begin{pmatrix} \frac{\partial H^*}{\partial x_1} & \frac{\partial H^*}{\partial x_2} & \frac{\partial H^*}{\partial x_3} & \frac{\partial H^*}{\partial y_1} & \frac{\partial H^*}{\partial y_2} & \frac{\partial H^*}{\partial y_3} \end{pmatrix} \begin{pmatrix} \partial H^*/\partial y_1 \\ \partial H^*/\partial y_2 \\ \partial H^*/\partial y_3 \\ -\partial H^*/\partial x_1 \\ -\partial H^*/\partial x_2 \\ -\partial H^*/\partial x_3 \end{pmatrix} = 0 \ .$$

So the candidates H^* and J are indeed integrals of the Hamiltonian system for the spherical pendulum that suffice the conditions of Liouville's Integrability Theorem. There is a certain property that integrals also have.

Theorem 5.4 ***Theorem 5.5***: *The Poisson-bracket $\{H, J\}$ is also an integral.*

Proof: According to the Jacobi-identity,

$$\{\{H, J\}, H\} = \{H, \{J, H\}\} + \{J, \{H, H\}\} = 0 + 0 = 0 \ .$$

Theorem 5.5 *Let $f \in C^\infty(M)$ for some $2N$-dimensional space M. Then $f(H, J)$ is also an integral.*

Proof: We have to show that $\{f(H, J), H\} = 0$ by the definition of an integral. According to the definition of the standard Poisson bracket,

$$\{f(H, J), H\} = \sum_{i=1}^{N} \Big(\frac{\partial f}{\partial q_i} \frac{\partial H}{\partial p_i} - \frac{\partial f}{\partial p_i} \frac{\partial H}{\partial q_i} \Big) \ . \tag{5}$$

Now by the Chain rule we get

$$\begin{aligned}
\frac{\partial f}{\partial q_i} &= \frac{\partial f}{\partial H} \frac{\partial H}{\partial q_i} + \frac{\partial f}{\partial J} \frac{\partial J}{\partial q_i} \\
\frac{\partial f}{\partial p_i} &= \frac{\partial f}{\partial H} \frac{\partial H}{\partial p_i} + \frac{\partial f}{\partial J} \frac{\partial J}{\partial p_i}
\end{aligned}$$

So substituting this in equation (5) gives

$$\begin{aligned}
\{f(H, J), H\} &= \sum_{i=1}^{N} \left(\frac{\partial H}{\partial p_i} \Big(\frac{\partial f}{\partial H} \frac{\partial H}{\partial q_i} + \frac{\partial f}{\partial J} \frac{\partial J}{\partial q_i} \Big) - \frac{\partial H}{\partial q_i} \Big(\frac{\partial f}{\partial H} \frac{\partial H}{\partial p_i} + \frac{\partial f}{\partial J} \frac{\partial J}{\partial p_i} \Big) \right) \\
&= \frac{\partial f}{\partial J} \sum_{i=1}^{N} \Big(\frac{\partial H}{\partial p_i} \frac{\partial J}{\partial q_i} - \frac{\partial H}{\partial q_i} \frac{\partial J}{\partial p_i} \Big) \\
&= \frac{\partial f}{\partial J} \{J, H\} = -\frac{\partial f}{\partial J} \{H, J\} = 0
\end{aligned}$$

So a smooth function f of integrals H and J is also an integral. However, because $f(H, J)$ is dependent on the integrals H and J it is never an independent integral. So it does not suffice Liouville's Integrability Theorem.

5.3 Flow and symmetries

Let the Hamiltonian vector field of J be denoted by X_J.
So

$$X_J = \begin{pmatrix} \frac{\partial J}{\partial y_1} \\ \frac{\partial J}{\partial y_2} \\ \frac{\partial J}{\partial y_3} \\ -\frac{\partial J}{\partial x_1} \\ -\frac{\partial J}{\partial x_2} \\ -\frac{\partial J}{\partial x_3} \end{pmatrix} = \begin{pmatrix} -x_2 \\ x_1 \\ 0 \\ -y_2 \\ y_1 \\ 0 \end{pmatrix}.$$

If the Hamiltonian system is completely integrable, then the Hamiltonian vector fields X_{H^*} and X_J commute with each other. Furthermore, they are tangent to and independent at the level sets $L_{c_1} = \{H = c_1\}$ and $L_{c_2} = \{J = c_2\}$ for some $c_1, c_2 \in \mathbb{R}$.
It is also true that solutions are mapped from X_{H^*} to X_{H^*} by X_J [4]. In order to bring the latter more into perspective, a few concepts have to be introduced.

Definition 5.6 (Flow) *Let $\psi : \mathbb{R} \times \mathbb{R}^3 \times \mathbb{R}^3 \to \mathbb{R}^6$ be the map given by $\psi(t, x_0, y_0) = (x(t), y(t))$, where $(x(t), y(t))$ is the solution of the vector field X_F with initial value (x_0, y_0) and with F the Hamiltonian.*
*Then the map $\psi_t : \mathbb{R}^3 \times \mathbb{R}^3 \to \mathbb{R}^6$, given by $\psi_t^F(x, y) = \psi(t, x, y)$ is called the **flow** of the vector field X_F.*

This basically means that a point on the solution curve of the vector field is mapped to another point on the same curve per time t.

Definition 5.7 (Symmetry) *Let $f \in C^\infty(M)$ be a smooth function.*
*A **symmetry** ψ is a map that leaves a function unchanged: $\psi \circ f = f$.*

Let the flow on the Hamiltonian vector field X_J be denoted by $\varphi_t^J : \mathbb{R}^3 \times \mathbb{R}^3 \to \mathbb{R}^6$, with φ_t^J given by

$$\varphi_t^J = \begin{pmatrix} \cos(t) & \sin(t) & 0 & 0 & 0 & 0 \\ -\sin(t) & \cos(t) & 0 & 0 & 0 & 0 \\ 0 & 0 & 1 & 0 & 0 & 0 \\ 0 & 0 & 0 & \cos(t) & \sin(t) & 0 \\ 0 & 0 & 0 & -\sin(t) & \cos(t) & 0 \\ 0 & 0 & 0 & 0 & 0 & 1 \end{pmatrix}.$$

It can be seen that this flow describes a rotation around the x_3-axis, as it leaves x_3 and y_3 in its place and x_1 and x_2 are described by trigonometric functions that describe circles.
Now because $\{H^*, J\} = 0$, it follows that φ_t^J is for each t a symmetry of X_{H^*}. In conclusion, if $\{(x(t), y(t)) | t \in \mathbb{R}\}$ is a solution curve of X_{H^*}, then $\{\varphi_t^J(x(t), y(t)) | t \in \mathbb{R}\}$ is a solution curve as well.
Now φ_t^J is also a so called Poisson-map.

Definition 5.8 (Poisson-map) *A map ψ is called a **Poisson-map** if for each $f, g \in C^\infty(M)$ the identity $\{f \circ \psi, g \circ \psi\} = \{f, g\} \circ \psi$ holds. Or in other words, if the map commutes with the bracket.*

If φ_t^J is a symmetry of H^*, then the next identity holds.

$$\{z \circ \varphi_t^J, H^* \circ \varphi_t^J\}(x) = \{z \circ \varphi_t^J, H^*\}(x) = \frac{d}{dt}(z \circ \varphi_t^J) = \{z, H^*\}(\varphi_t^J(x)) \ .$$

If the flows on the Hamiltonian vector fields X_{H^*} and X_J will leave the surfaces $R_1 = x_1^2 + x_2^2 + x_3^2 - 1 = 0$ and $R_2 = x_1y_1 + x_2y_2 + x_3y_3$ unchanged, this means that solutions on the 2-sphere do not change either. This means that the symmetries of X_{H^*} and X_J indeed map solution curves to solution curves. To prove that this is the case, we have to check the Poisson-brackets $\{H, R_1\}$, $\{H, R_2\}$, $\{J, R_1\}$ and $\{J, R_2\}$.

$$\begin{aligned}
\{H, R_1\} &= \{H, x_1^2 + x_2^2 + x_3^2 - 1\} \\
&= \{H, x_1^2\} + \{H, x_2^2\} + \{H, x_3^2\} - \{H, 1\} \\
&= 2(x_1\{H, x_1\} + x_2\{H, x_2\} + x_3\{H, x_3\}) \\
&= 2\Big(x_1\frac{\partial H}{\partial y_1} + x_2\frac{\partial H}{\partial y_2} + x_3\frac{\partial H}{\partial y_3}\Big) \\
&= 2(x_1y_1 + x_2y_2 + x_3y_3) = 0
\end{aligned}$$

$$\begin{aligned}
\{H, R_2\} &= \{H, x_1y_1 + x_2y_2 + x_3y_3\} \\
&= \{H, x_1y_1\} + \{H, x_2y_2\} + \{H, x_3y_3\} \\
&= x_1\{H, y_1\} + y_1\{H, x_1\} + x_2\{H, y_2\} + y_2\{H, x_2\} + x_3\{H, y_3\} + y_3\{H, x_3\} \\
&= -x_1\frac{\partial H}{\partial x_1} + y_1\frac{\partial H}{\partial y_1} - x_2\frac{\partial H}{\partial x_2} + y_2\frac{\partial H}{\partial y_2} - x_3\frac{\partial H}{\partial x_3} + y_3\frac{\partial H}{\partial y_3} \\
&= x_1(x_3 - y_1^2 + y_2^2 + y_3^2)x_1 + y_1^2 \\
&+ x_2(x_3 - y_1^2 + y_2^2 + y_3^2)x_2 + y_2^2 \\
&+ x_3(-1 + (x_3 - y_1^2 + y_2^2 + y_3^2)x_3) + y_3^2 \\
&= -(x_1^2 + x_2^2 + x_3^2)(y_1^2 + y_2^2 + y_3^2) + (y_1^2 + y_2^2 + y_3^2) + (x_1^2 + x_2^2 + x_3^2)x_3 - x_3 \\
&= 0
\end{aligned}$$

$$\begin{aligned}
\{J, R_1\} &= \{J, x_1^2 + x_2^2 + x_3^2 - 1\} \\
&= \{x_1y_2 - x_2y_1, x_1^2 + x_2^2 + x_3^2 - 1\} \\
&= \{x_1y_2, x_1^2\} + \{x_1y_2, x_2^2\} + \{x_1y_2, x_3^2\} - \{x_1y_2, 1\} - \{x_2y_1, x_1^2\} - \{x_2y_1, x_2^2\} - \{x_2y_1, x_3^2\} + \{x_1y_2, 1\} \\
&= -2(x_1\{x_1y_2, x_1\} + x_2\{x_1y_2, x_2\} + x_3\{x_1y_2, x_3\} - x_1\{x_2y_1, x_1\} - x_2\{x_2y_1, x_2\} - x_3\{x_2y_1, x_3\}) \\
&= -2(x_1^2\{y_2, x_1\} + x_1y_2\{x_1, x_1\} + x_1x_2\{y_2, x_2\} + x_2y_2\{x_1, x_2\} + x_1x_3\{y_2, x_3\} \\
&+ x_3y_2\{x_1, x_3\} - x_1x_2\{y_1, x_1\} - x_1y_1\{x_2, x_1\} - x_2^2\{y_1, x_2\} \\
&- x_2y_1\{x_2, x_2\} - x_2x_3\{y_1, x_3\} - x_3y_1\{x_2, x_3\} \\
&= -2(-x_1x_2 + x_1x_2) \text{ (because } \{x_i, y_j\} = \delta_{i,j}) \\
&= 0
\end{aligned}$$

$$\begin{aligned}
\{J, R_2\} &= \{J, x_1y_1 + x_2y_2 + x_3y_3\} \\
&= \{x_1y_2, x_1y_1\} + \{x_1y_2, x_2y_2\} + \{x_1y_2, x_3y_3\} - \{x_2y_1, x_1y_1\} - \{x_2y_1, x_2y_2\} - \{x_2y_1, x_3y_3\} \\
&= x_1\{y_2, x_1y_1\} + y_2\{x_1, x_1y_1\} + x_1\{y_2, x_2y_2\} + y_2\{x_1, x_2y_2\} + x_1\{y_2, x_3y_3\} + y_2\{x_1, x_3y_3\} \\
&- x_2\{y_1, x_1y_1\} - y_1\{x_2, x_1y_1\} - x_2\{y_1, x_2y_2\} - y_1\{x_2, x_2y_2\} - x_2\{y_1, x_3y_3\} - y_1\{x_2, x_3y_3\} \\
&= -x_1^2\{y_2, y_1\} - x_1y_1\{y_2, x_1\} - x_1y_2\{x_1, y_1\} - y_1y_2\{x_1, x_1\} - x_1x_2\{y_2, y_2\} - x_1y_2\{y_2, x_2\} \\
&- x_2y_2\{x_1, y_2\} - y_2^2\{x_1, x_2\} - x_1x_3\{y_2, y_3\} - x_1y_3\{y_2, x_3\} - y_2x_3\{x_1, y_3\} - y_2y_3\{x_1, x_3\} \\
&+ x_1x_2\{y_1, y_1\} + x_2y_1\{y_1, x_1\} + x_1y_1\{x_2, y_1\} + y_1^2\{x_2, x_1\} + x_2^2\{y_1, y_2\} + x_2y_2\{y_1, x_2\} \\
&+ x_2y_1\{x_2, y_2\} + y_1y_2\{x_2, x_2\} + x_2x_3\{y_1, y_3\} + x_2y_3\{y_1, x_3\} + x_3y_1\{x_2, y_3\} + y_1y_3\{x_2, x_3\} \\
&= -x_1y_2 + x_1y_2 - x_2y_1 + x_2y_1 \text{ (because } \{x_i, y_j\} = \delta_{i,j}) \\
&= 0
\end{aligned}$$

So the Poisson-brackets are all zero, which means that the symmetries of $X_{H^*}$and X_J indeed map solution curves to solution curves. If the curves of $X_{H^*}$and X_J coincide, the solutions of the Hamiltonian equations are called periodic solutions. In the next section a way to find these solutions will be presented.

6 Energy momentum mapping

In this section we consider the Energy momentum mapping to study the system

$$EM : TS^2 \subseteq T\mathbb{R}^3 \to \mathbb{R}^2 :$$
$$(x, y) \to (H^*, J) = \left(\frac{1}{2}(y_1^2 + y_2^2 + y_3^2) + x_3, x_1 y_2 - x_2 y_1\right) .$$

As determined in section 5, these H^* and J are integrals of the Hamiltonian vector field X_{H^*} and they commute almost everywhere by Liouville's Integrability theorem. The vector fields of H^* and J are by the same theorem almost everywhere independent, except for sets of Lebesgue-measure zero. The interesting places to investigate are thus the points where the integrals are dependent of each other. It is in these points where the critical values of EM are found. This implies that at these points Liouville's Integrability Theorem no longer holds. Important cases to keep in mind also are the special cases $\nabla H^* = 0$ and $\nabla J = 0$. The solutions to these equations are called the stationary solutions. This implies that the phase space no longer will be described by invariant tori, but solutions that are called periodic solutions together with the stationary solutions. For the sake of completion it is thus necessary to investigate these critical values.
In mathematical terms, we have to find the solutions of

$$\begin{aligned} \nabla H^* &= 0 , \\ \nabla J &= 0 , \\ \nabla H^* + \lambda \nabla J &= 0 . \end{aligned}$$

Here $\lambda \in \mathbb{R}$ is taken, but normally we are not interested in the value of λ, because this will not give us information about the solutions.
The Hamilton equations $\frac{dx}{dt} = \frac{\partial H^*}{\partial y}$ and $\frac{dy}{dt} = -\frac{\partial H^*}{\partial x}$ yield together with the last two equations of section 4 the following equation,

$$\nabla H^* = \begin{pmatrix} -(x_3 - |y|^2)x_1 \\ -(x_3 - |y|^2)x_2 \\ 1 - (x_3 - |y|^2)x_3 \\ y_1 \\ y_2 \\ y_3 \end{pmatrix} .$$

Now ∇J is equal to

$$\nabla J = \begin{pmatrix} y_2 \\ -y_1 \\ 0 \\ -x_2 \\ x_1 \\ 0 \end{pmatrix} .$$

The stationary solutions are described in section 7.1.
To determine the periodic solutions, the following system has to be solved,

$$\begin{aligned} -(x_3 - |y|^2)x_1 + \lambda y_2 &= 0 , \\ -(x_3 - |y|^2)x_2 - \lambda y_1 &= 0 , \\ 1 - (x_3 - |y|^2)x_3 &= 0 , \\ y_1 - \lambda x_2 &= 0 , \\ y_2 + \lambda x_1 &= 0 , \\ y_3 &= 0 . \end{aligned}$$

Furthermore there are 2 additional constraints

$$|x|^2 = x_1^2 + x_2^2 + x_3^2 = 1 \ ,$$
$$< x, y >= x_1 y_1 + x_2 y_2 + x_3 y_3 = 0 \ .$$

The purpose now is to find expressions that express certain combinations of variables in other variables, but in such a way that these combinations are easy to work with and important for the rest of the approach.
From the last equation $y_3 = 0$ in the system it follows that $|y|^2 = y_1^2 + y_2^2$ and $x_1y_1 + x_2y_2 = 0$. Now J satisfies the identity

$$(x_1y_1 + x_2y_2)^2 + J^2 = (x_1^2 + x_2^2)(y_1^2 + y_2^2) \ .$$

From here it follows that

$$J^2 = (x_1^2 + x_2^2)(y_1^2 + y_2^2) \ .$$

Combining this with the equation $x_1^2 + x_2^2 + x_3^2 = 1$ gives

$$J^2 = (1 - x_3^2)(y_1^2 + y_2^2) \ .$$

The third equation $1 - (x_3 - |y|^2)x_3 = 0$ gives

$$y_1^2 + y_2^2 = \frac{x_3^2 - 1}{x_3} \ .$$

So until now the next expressions for H^* and J are found,

$$\begin{aligned} H^* = \frac{x_3^2 - 1}{2x_3} + x_3 = \frac{3x_3^2 - 1}{2x_3} \ , \\ J^2 = -\frac{(1 - x_3^2)^2}{x_3} \ . \end{aligned} \tag{6}$$

Here are H^* and J essentially parametrized by x_3. The next step is to find the explicit relation between H^* and J rather than just a parametrization in the variable x_3. First, equations (6) are rewritten as

$$\begin{aligned} 3x_3^2 - 2x_3H^* - 1 = 0 \ , \\ x_3^4 - x_3J^2 - 2x_3^2 + 1 = 0 \ . \end{aligned} \tag{7}$$

These are polynomials in x_3, so it is interesting to look now for the resultant of these polynomials.

Definition 6.1 *A **Resultant** is a polynomial expression of the coefficients of two polynomials, which is equal to zero if and only if the polynomials have a common root.[5]*

Equations (7) having a common root means that x_3 in the first equation is the same as the x_3 in the second equation. Now keep in mind that this does not hold for points where the integrals H^* and J are independent of each other. So this characterises that the points where the resultant is zero are critical values of the Energy momentum mapping. Computing the resultant of the equations (7) gives

$$27J^4 + (72H^* - 8(H^*)^3)J^2 + 32(H^*)^2 - 16(H^*)^4 - 16 = 0 \ .$$

Solving this equation for J gives

$$J = \pm\frac{2}{3\sqrt{3}}\sqrt{9H^* - (H^*)^3 + \sqrt{((H^*)^2 + 3)^3}} \ .$$

The positive J is seen in figure 3. Likewise, the negative J is the mirroring of the positive graph in the H^*-axis.
Again, the derived relations between $x_1, x_2, x_3, y_1, y_2, y_3, H^*$ and J only hold on the graphs, not in the area they enclose.

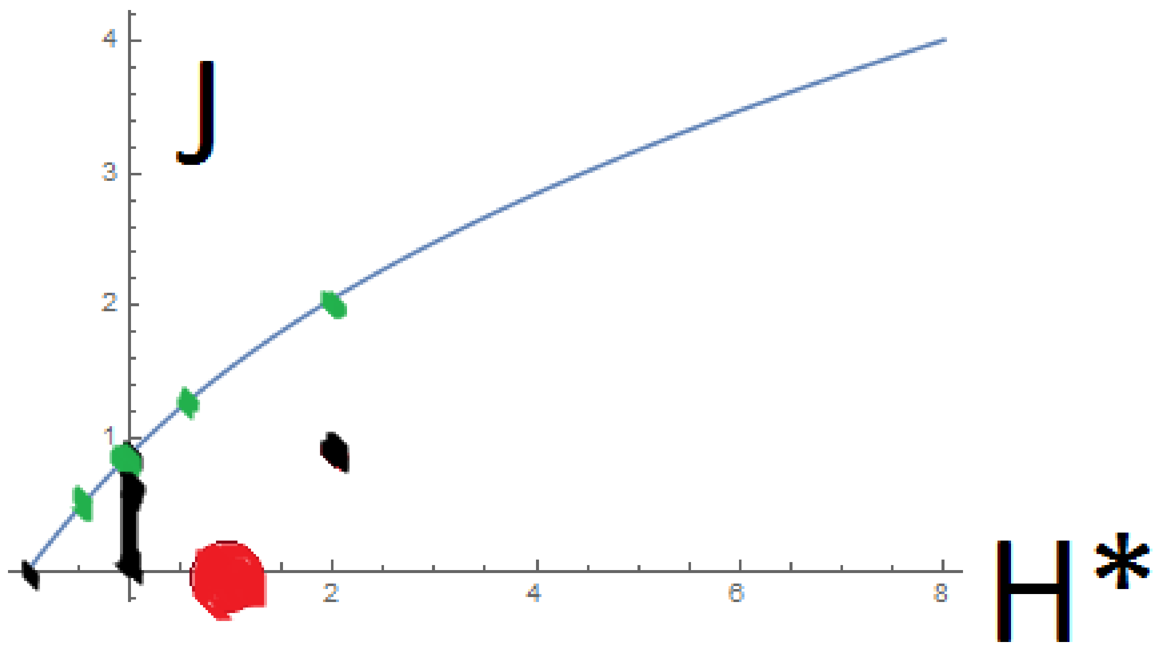

Figure 3: J as a function of H^*. The coloured points are points whose counter-images are investigated

7 Classification of solutions

In this section there will be elaborated on the four different types of solutions.

- Stationary solutions (For points $(H^*, J) = (-1, 0)$ and $(H^*, J) = (1, 0)$)
- Periodic solutions (Solutions on the branches)
- Invariant tori (Solutions in between the branches)
- Pinched Torus (For points nearby the point $(H^*, J) = (1, 0)$)

7.1 Stationary solutions

The claim is that the points $(H^*, J) = (-1, 0)$ and $(H^*, J) = (1, 0)$ are singular points of the energy-momentum Mapping. Indeed, if the equations $\nabla H^* = 0$ and $\nabla J = 0$ are regarded, it follows immediately that $x_1 = x_2 = y_1 = y_2 = y_3 = 0$ and $1 - x_3^2 = 0$, so $x_3 = \pm 1$. The stationary solutions are thus $(0, 0, \pm 1, 0, 0, 0)$ in the phase space.
After substituting these solutions in the equations

$$\frac{1}{2}(y_1^2 + y_2^2 + y_3^2) + x_3 = H^* \ ,$$

$$x_1 y_2 - x_2 y_1 = J \ ,$$

it follows that $(H^*, J) = (\pm 1, 0)$ are the critical values of the Energy momentum mapping for which the counter-images contain the stationary solutions in the phase space. The flow on both solutions describe the movement of the pendulum. This movement comes down to resting in the points $(0, 0, -1, 0, 0, 0)$ if $(H^*, J) = (-1, 0)$ and $(0, 0, 1, 0, 0, 0)$ if $(H^*, J) = (1, 0)$ in the phase space. It is intuitively clear that the solution $(0, 0, -1, 0, 0, 0)$ is a stable solution and the solution $(0, 0, 1, 0, 0, 0)$ is an unstable solution.

7.2 Periodic Solutions

The counter-images of points (H^*, J) on the branches are to be determined now.
In order to do this, the system

$$\begin{aligned} \frac{1}{2}(y_1^2+y_2^2+y_3^2)+x_3 &= H^* \ , \\ x_1y_2-x_2y_1 &= J \ , \\ x_1^2+x_2^2 &= 1-x_3^2 \ , \\ x_1y_1+x_2y_2+x_3y_3 &= 0 \ , \end{aligned} \tag{8}$$

has to be used together with the relations derived from the equations that belong to the Energy momentum mapping, which are

$$\begin{aligned} H^* &= \frac{3x_3^2-1}{2x_3} \ , \\ J^2 &= -\frac{(1-x_3^2)^2}{x_3} \ , \\ y_1^2+y_2^2 &= \frac{x_3^2-1}{x_3} \ , \\ y_3 &= 0 \ . \end{aligned}$$

A first step is to determine x_3 as function of H^* in order to compute the radii of the circles $x_1^2+x_2^2$ and $y_1^2+y_2^2$. This yields

$$3x_3^2-2x_3H^*-1=0 \ .$$

So

$$x_3=\frac{2H^*\pm\sqrt{4(H^*)^2+12}}{6}=\frac{1}{3}H^*\pm\frac{1}{3}\sqrt{(H^*)^2+3} \ .$$

Now it is interesting to know which of the two values for x_3 is appropriate for which value of H^*. There are always both a positive and a negative value for x_3, because $(\sqrt{(H^*)^2+3})/3 > H^*/3$ and $(\sqrt{(H^*)^2+3})/3 > 0$.
So the $+$ in the solution of x_3 always gives a positive value and the $-$ always gives a negative value.
From the identity $y_1^2+y_2^2=(x_3^2-1)x_3^{-1}$ it immediately follows that x_3 has to be negative. Otherwise the left hand side would be negative, which gives a contradiction. This is all regardless of the value of H^*
Now that x_3 is established, it can easily be computed that $y_1^2+y_2^2=(x_3^2-1)x_3^{-1}$ and $x_1^2+x_2^2=1-x_3^2$ and the periodic solution described by 2 circles follows.

As an example H^* and J expressed in x and y are taken for the point on the branch that intersects the positive J-axis. With a calculation (which consists of substituting $H^*=0$ in the equation $J=\pm(2\sqrt{9H^*-(H^*)^3+\sqrt{((H^*)^2+3)^3}})/(3\sqrt{3})$ it can be shown that this point is $(H^*,J)=(0,\frac{2}{3}\sqrt{\sqrt{3}})$. So substituting these values in the first two equations of the system (8) gives

$$\begin{aligned} \frac{1}{2}(y_1^2+y_2^2+y_3^2)+x_3 &= 0 \ , \\ x_1y_2-x_2y_1 &= \frac{2}{3}\sqrt{\sqrt{3}} \ . \end{aligned}$$

It is established earlier that x_3 has to be negative, from which it follows that $-1\le x_3<0$. Then it is the case that $x_3=H^*/3-(\sqrt{(H^*)^2+3})/3=-\sqrt{3}/3$. Substituting this value for x_3 in the equation $y_1^2+y_2^2=(x_3^2-1)x_3^{-1}$ gives $y_1^2+y_2^2=2\sqrt{3}/3$. And substituting this value for x_3 also in

the equation $x_1^2 + x_2^2 = 1 - x_3^2$ gives $x_1^2 + x_2^2 = 2/3$. This yields a periodic solution described by 2 circles, which corresponds to a horizontal circle in the configuration space.
To give more examples and to show the difference between periodic solutions that are contained by the flow on the counter-images of various points on the branches in the (H^*, J)-plane, the next points have been chosen:

- Point $(H^*, J) = (-0.5, 0.469)$.
  Then $x_3 = H^*/3 - (\sqrt{(H^*)^2 + 3})/3 = -0.768$.
  Furthermore it turns out that $y_1^2 + y_2^2 = 0.535$ and $x_1^2 + x_2^2 = 0.411$.
- Point $(H^*, J) = (0.5, 1.231)$.
  Then $x_3 = H^*/3 - (\sqrt{(H^*)^2 + 3})/3 = -0.434$.
  Furthermore it turns out that $y_1^2 + y_2^2 = 1.869$ and $x_1^2 + x_2^2 = 0.811$.
- Point $(H^*, J) = (2, 2.056)$.
  Then $x_3 = H^*/3 - (\sqrt{(H^*)^2 + 3})/3 = -0.215$.
  Furthermore it turns out that $y_1^2 + y_2^2 = 4.431$ and $x_1^2 + x_2^2 = 0.954$

It can be noticed that how bigger H^* becomes, how bigger the circle $y_1^2 + y_2^2$ becomes and how closer $x_1^2 + x_2^2$ gets to 1 and thus how closer x_3 gets to 0. This is in agreement with the earlier established fact that $-1 \leq x_3 < 0$.
Because we can easily calculate the radii of the circles $x_1^2 + x_2^2$ and $y_1^2 + y_2^2$ with the value of x_3 for points on the branches and because the equality $J = x_1y_2 - x_2y_1$ holds, we can find initial values for x and y in order to solve the system of differential equations numerically. Now let $x_1^2 + x_2^2 = c_1$ and $y_1^2 + y_2^2 = c_2$ with $c_1, c_2 > 0$. Then $x_1 = \sqrt{c_1 - x_2^2}$ and $y_1 = \sqrt{c_2 - y_2^2}$ and

$$\begin{aligned}
&y_2\sqrt{c1 - x_2^2} - x_2\sqrt{c_2 - y_2^2} = J\ , \\
&y_2^2(c_1 - x_2^2) - 2Jy_2\sqrt{c_1 - x_2^2} + J^2 = x_2^2(c_2 - y_2^2)\ , \\
&c_1y_2^2 - 2Jy_2\sqrt{c_1 - x_2^2} + J^2 - c_2x_2^2 = 0\ , \\
&y_2 = \frac{1}{2c_1}\left(2J\sqrt{c_1 - x_2^2} \pm \sqrt{4x_2^2(c_1c_2 - J^2)}\right)\ .
\end{aligned} \tag{9}$$

It is noticed earlier that $J^2 = (x_1^2 + x_2^2)(y_1^2 + y_2^2) = c_1c_2$.
The last equation of equations (9) then reduces to $y_2 = (J\sqrt{c_1 - x_2^2})c_1^{-1}$.
So if there is given some $x_2 \in [0, \sqrt{c_1}]$, then x_1, y_1 and y_2 are fixed by that choice. In Mathematica a program is made to determine the solutions of $x_1(t), x_2(t), x_3(t)$ in the configuration space both parametrically and as functions of t.
After having solved the system, a parametric 3D-plot is made of the functions $x_1(t), x_2(t)$ and $x_3(t)$ and this indeed corresponds to a circle (see Figure 4). Furthermore, a plot of these functions against the time t is made (see Figure 5). From here it is obvious that x_1 and x_2 are a cosine and a sine respectively with amplitude $\sqrt{c_1}$ and a certain period ω. As expected, x_3 is constant along t.

$$\begin{aligned}
x_1(t) &= \sqrt{c_1}\cos(\omega t)\ , \\
x_2(t) &= \sqrt{c_1}\sin(\omega t)\ , \\
x_3(t) &= c,\ c \in [-1, 1]\ .
\end{aligned}$$

The example used for the making of the graphs is the point $(H^*, J) = (0, \frac{2}{3}\sqrt{\sqrt{3}})$. But for other points on the branches in the (H^*, J)-plane the same kind of results hold.

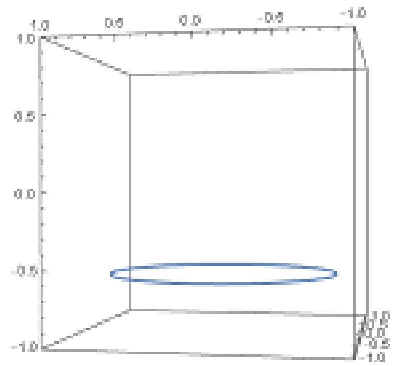

Figure 4: Parametric plot of $x_1(t)$, $x_2(t)$ and $x_3(t)$ for $(H^*, J) = (0, 0.877)$

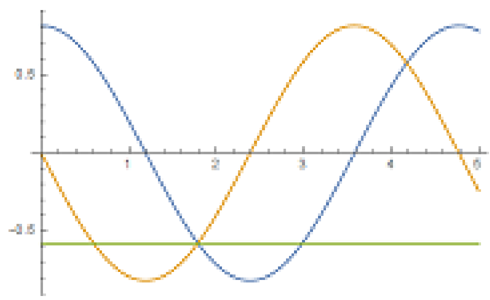

Figure 5: Time series plot of $x_1(t)$ (blue), $x_2(t)$ (orange) and $x_3(t)$ (green) for $(H^*, J) = (0, 0.877)$ against the time t

7.3 Invariant Tori

The counter-images of all points between the branches are by Liouville's Integrability theorem invariant tori, because the gradients of the integrals H^* and J are there independent of each other. Furthermore, the level sets $\{H^* = c_1\} \cap \{J = c_2\}$ are compact by the following reasoning. By the equality $x_1^2 + x_2^2 + x_3^2 = 1$ it follows directly that x_1, x_2 and x_3 are bounded. Then on the level set $(y_1^2 + y_2^2 + y_3^2)/2 + x_3 = c_1$ the term $(y_1^2 + y_2^2 + y_3^2)/2$ is bounded also.
So the level set $\{H^* = c_1\}$ is $\forall x \in S^2$ closed and bounded and thus compact. So the intersection $\{H^* = c_1\} \cap \{J = c_2\}$ is also compact.
The theorem then says that the phase space is foliated with invariant tori near a regular point. The flow on these tori determines the movement of the pendulum in the phase space. In the configuration space the movement of the pendulum then translates to a simultaneous swinging and rotating around the x_3-axis.
Because the invariant surfaces $\{H^* = c_1\} \cap \{J = c_2\}$ are bounded, the counter-images of points on the outside of the branches are not invariant tori. Only points in the (H^*, J)-plane that are locate in the area enclosed by the branches are thus to be investigated.
In the following part of this subsection the counter-images of the points in between the branches in the (H^*, J)-plane will be explored. The integrals H^* and J will be treated as if they were variables. In this way a general approach can be made in order to determine the solutions x and y in the phase space.

For this approach we have to choose initial values for x ad y such that the next system holds,

$$\begin{aligned} \frac{1}{2}(y_1^2+y_2^2+y_3^2)+x_3 &= H^* \ , \\ x_1y_2-x_2y_1 &= J \ , \\ x_1^2+x_2^2+x_3^2 &= 1 \ , \\ x_1y_1+x_2y_2+x_3y_3 &= 0 \ . \end{aligned}$$

Different initial values for x and y result in different solutions, but all of these solutions are described by the same flow on a torus. So the trajectory of the solution stays the same, but the orientation is different. This holds for all solutions that are explored in not only this subsection, but also the next one.

A way to solve the problem is to express x_1, x_2 and x_3 in terms of y_1, y_2 and y_3 and then to choose two of the last three quantities wisely such that the system still holds.

The second equation gives

$$x_1 = \frac{J+x_2y_1}{y_2} \ .$$

Substituting this in the fourth equation then gives

$$\begin{aligned} Jy_1+x_2y_1^2+x_2y_2^2+x_3y_2y_3 &= 0 \ , \\ x_2 &= \frac{-x_3y_2y_3-Jy_1}{y_1^2+y_2^2} \ . \end{aligned}$$

We have as intermediate results

$$\begin{aligned} x_1 &= \frac{J+x_2y_1}{y_2} \ , \\ x_2 &= \frac{-x_3y_2y_3-Jy_1}{y_1^2+y_2^2} \ . \end{aligned}$$

Now $x_3 = H^* - (y_1^2+y_2^2+y_3^2)/2$. Putting $z = y_1^2+y_2^2+y_3^2$ and substituting this in the previous expressions gives

$$\begin{aligned} x_1 &= \frac{Jy_2}{y_1^2+y_2^2} + \frac{y_1y_3\left(\frac{1}{2}z-H^*\right)}{y_1^2+y_2^2} \ , \\ x_2 &= -\frac{Jy_1}{y_1^2+y_2^2} + \frac{y_2y_3\left(\frac{1}{2}z-H^*\right)}{y_1^2+y_2^2} \ , \\ x_3 &= H^* - \frac{1}{2}z \ . \end{aligned} \tag{10}$$

Substituting these expressions in the third equation $x_1^2+x_2^2+x_3^2=1$ gives

$$\begin{aligned} &\frac{J^2y_2^2}{y_1^2+y_2^2} + \frac{Jy_1y_2y_3\left(\frac{1}{2}z-2H^*\right)}{(y_1^2+y_2^2)^2} + \frac{y_1^2y_3^2\left(\frac{1}{2}z-H^*\right)^2}{(y_1^2+y_2^2)^2} \\ &+ \frac{J^2y_1^2}{y_1^2+y_2^2} - \frac{Jy_1y_2y_3\left(\frac{1}{2}z-2H^*\right)}{(y_1^2+y_2^2)^2} + \frac{y_2^2y_3^2\left(\frac{1}{2}z-H^*\right)^2}{(y_1^2+y_2^2)^2} \\ &+ \left(H^*-\frac{1}{2}z\right)^2 = 1 \ . \end{aligned}$$

After some rearranging and eliminating this equation reduces to

$$\frac{J^2+z\left(\frac{1}{2}z-H^*\right)^2}{y_1^2+y_2^2} = 1 \ . \tag{11}$$

It follows that $y_1^2 + y_2^2 = J^2 + z\Big(\frac{1}{2}z - H^*\Big)^2$.
Add y_3^2 to both the right and left side to get

$$\frac{1}{4}z^3 - H^*z^2 + ((H^*)^2 - 1)z + J^2 + y_3^2 = 0 \ .$$

Now there are some points in the (H^*, J)-plane that are interesting to investigate:

- Points on the line segment $l : \{H^* = 0, -\frac{2}{3}\sqrt{\sqrt{3}} < J < \frac{2}{3}\sqrt{\sqrt{3}}\}$ are investigated. This value for H^* is chosen such tht a comparison can be made with the earlier investigated point $(H^*, J) = (0, \frac{2}{3}\sqrt{\sqrt{3}})$. The interesting thing to know is how the movement of the pendulum changes as one goes over this line. The next three points are chosen: $(H^*, J) = (0, 0)$, $(H^*, J) = (0, 0.435)$ and $(H^*, J) = (0, 0.87)$.
- Points for which it holds that $H^* > 1$ are investigated. Such points are expected to give more wilder results as the ones on the line l. As an example the point $(H^*, J) = (2, 1)$ is taken.
- Points nearby the point $(H^*, J) = (1, 0)$ are investigated. Included are the points $(H^*, J) = (0.99, 0)$ and $(H^*, J) = (1.01, 0)$. These points are saved for the next subsection about the pinched torus.

Point $(H^*, J) = (0, 0)$

First the point $(H^*, J) = (0, 0)$ is taken.
Now y_3 must be chosen such that z has non-negative solutions, because $z = y_1^2 + y_2^2 + y_3^2 \geq 0$.
If we take $y_3 = 0.5$, then z has a negative and two positive solutions, i.e.

$$z \approx -2.11491, \ z \approx 0.254102, \ z \approx 1.86081$$

We take $z \approx 1.86081$ as a solution. From this it follows that $y_1^2 + y_2^2 \approx 1.61081$. If we take $y_1 = 1$, then $y_2 \approx \sqrt{0.61081} \approx 0.781543$. These values for y_1, y_2 and y_3 are then substituted in the expressions (10) for x_1, x_2 and x_3 to give

$$\begin{aligned} x_1 &= 0.2888 \ , \\ x_2 &= 0.22571 \ , \\ x_3 &= -0.930405 \ , \\ y_1 &= 1 \ , \\ y_2 &= 0.781543 \ , \\ y_3 &= 0.5 \ . \end{aligned}$$

Unfortunately, the closed expressions for z are very cumbersome and complex moreover, so we were not able to put these expressions explicitly in Mathematica, but used only the approximations. The results are therefore slightly off, but not significantly much.
Putting these approximations in Mathematica and plotting the solutions results in Figures 6 and 7. It can be seen immediately in Figure 6 that the pendulum only swings up and down. This is the result of the fact that $J = 0$, because then the rotation around the x_3-axis vanishes. The solution of x_3 is not dependent on this, and will always move between -1 and 0, regardless of the initial values of y_1, y_2 and y_3, as can be seen in Figure 7. Moreover, it can be noted from the graphs of $x_1(t)$ and $x_2(t)$ in this Figure that the pendulum stays a few seconds in the neighbourhood of $x_3 = 0$.

Point $(H^*, J) = (0, 0.435)$

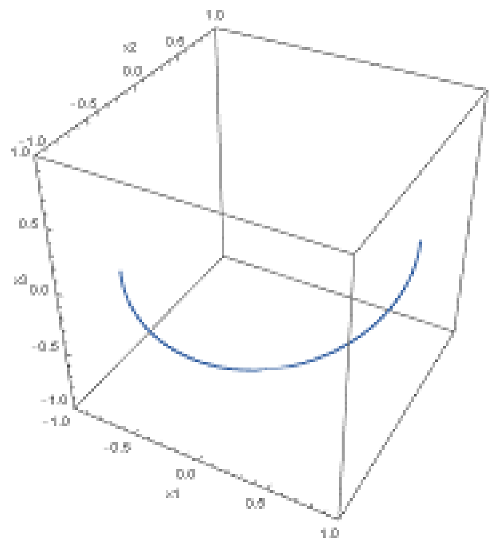

Figure 6: Parametric plot of $x_1(t)$, $x_2(t)$ and $x_3(t)$ for $(H^*, J) = (0, 0)$

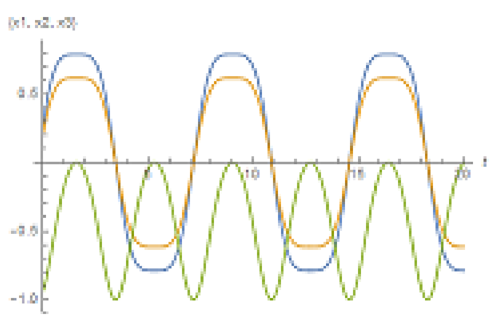

Figure 7: Time series plot of $x_1(t)$ (blue), $x_2(t)$ (beige) and $x_3(t)$ (green) for $(H^*, J) = (0, 0)$ against the time t

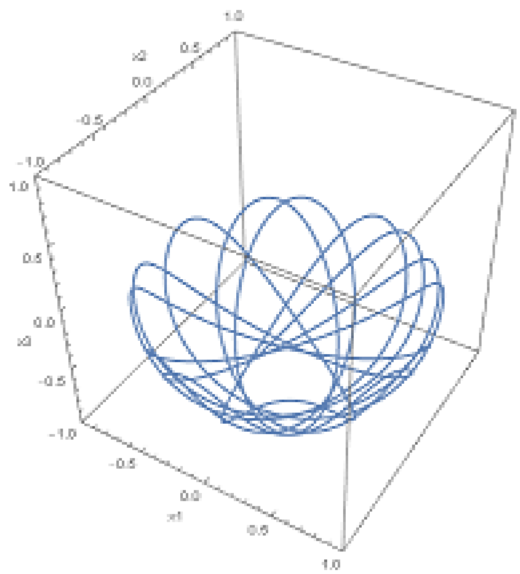

Figure 8: Parametric plot of $x_1(t)$, $x_2(t)$ and $x_3(t)$ for $(H^*, J) = (0, 0.435)$

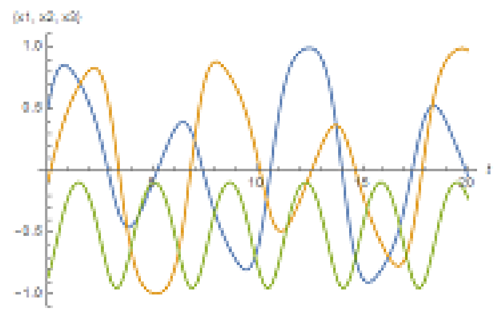

Figure 9: Time series plot of $x_1(t)$ (blue), $x_2(t)$ (beige) and $x_3(t)$ (green) for $(H^*, J) = (0, 0.435)$ against the time t

Going upwards on the line l, we take as an example the point halfway the line $(H^*, J) = (0, 0.435)$. Choosing $y_3 = 0.5$ and solving the equation $(z^3 - z + J^2 + y_3^2)/4 = 0$ again, but now for $J = 0.435$, gives as a solution $z \approx 1.72706$. Consequently we take $y_1 = 1$, so that $y_2 = \sqrt{1.47706} \approx 0.690695$. Plugging y_1, y_2 and y_3 in the expressions for x_1, x_2 and x_3 gives

$$\begin{aligned} x_1 &= 0.495726\ , \\ x_2 &= -0.0926042\ , \\ x_3 &= -0.86353\ , \\ y_1 &= 1\ , \\ y_2 &= 0.690695\ , \\ y_3 &= 0.5\ . \end{aligned}$$

Putting these approximations in Mathematica and plotting the solutions results in figures 8 and 9. Figures 8 and 9 show that the pendulum swings everywhere in the lower half of the sphere, but will not go above $x_3 = 0$, because $x_3(t)$ stays below zero as can be seen in figure 9. As it does not reach above $x_3 = 0$, the pendulum does not make turnovers.

Point $(H^*, J) = (0, 0.87)$

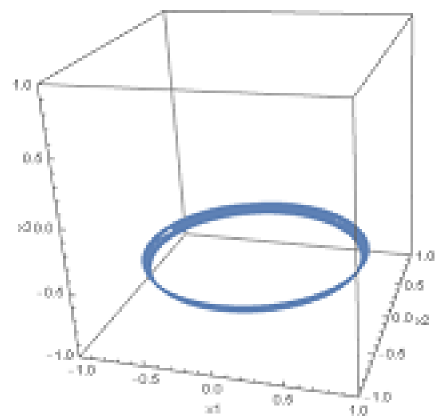

Figure 10: Parametric plot of $x_1(t)$, $x_2(t)$ and $x_3(t)$ for $(H^*, J) = (0, 0.87)$

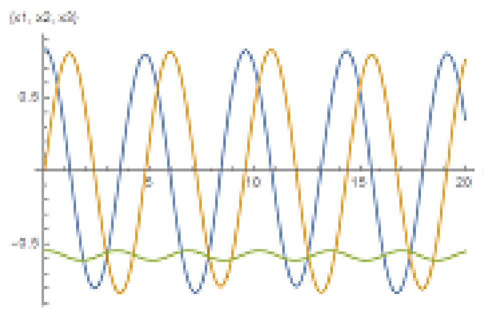

Figure 11: Time series plot of $x_1(t)$ (blue), $x_2(t)$ (beige) and $x_3(t)$ (green) for $(H^*, J) = (0, 0.87)$ against the time t

Going upwards again on the line l, we take as an example the point close to the branch $(H^*, J) = (0, 0.87)$.
Choosing $y_3 = 0.01$ and solving the equation $\frac{1}{4}z^3 - z + J^2 + y_3^2 = 0$ again, but now for $J = 0.87$, gives as a solution $z \approx 1.08781$. Consequently we take $y_1 = 0$, so that $y_2 = \sqrt{1.08771} \approx 1.04293$. Plugging y_1, y_2 and y_3 in the expressions for x_1, x_2 and x_3 gives

$$
\begin{aligned}
x_1 &= 0.834186 \ , \\
x_2 &= -0.00521515 \ , \\
x_3 &= -0.543905 \ , \\
y_1 &= 0 \ , \\
y_2 &= 1.04293 \ , \\
y_3 &= 0.01 \ .
\end{aligned}
$$

Putting these approximations in Mathematica and plotting the solutions results in Figures 10 and 11. It can be seen in Figures 10 and 11 that the pendulum almost moves in a circle, but with a regular oscillation of $x_3(t)$ around the value $-\sqrt{3}/3$, as was derived in the previous subsection.

Point $(H^*, J) = (2, 1)$

Another interesting type of point is the type where $H^* > 1$.
As an example the point $(H^*, J) = (2, 1)$ is taken.

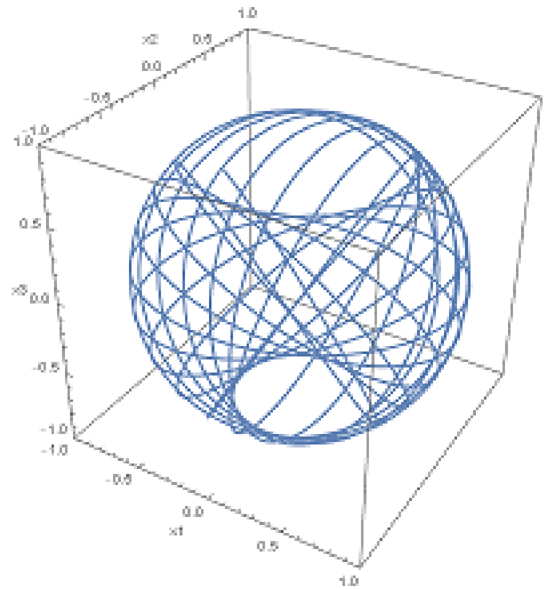

Figure 12: Parametric plot of $x_1(t)$, $x_2(t)$ and $x_3(t)$ for $(H^*, J) = (2, 1)$

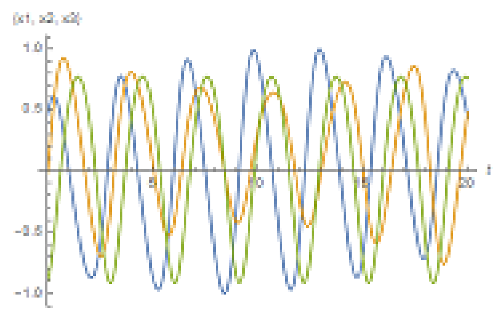

Figure 13: Time series plot of $x_1(t)$ (blue), $x_2(t)$ (beige) and $x_3(t)$ (green) for $(H^*, J) = (2, 1)$ against the time t

Using the same approach as on the line l, but now with $H^* = 2$ one gets $z = 5.77016$ and as initial values for x and y

$$
\begin{aligned}
x_1 &= 0.465314 \ , \\
x_2 &= -0.0107117 \ , \\
x_3 &= -0.88508 \ , \\
y_1 &= 1 \ , \\
y_2 &= 2.12607 \ , \\
y_3 &= 0.5 \ .
\end{aligned}
$$

Putting these approximations in Mathematica and plotting the solutions results in Figures 12 and 13. From Figures 12 and 13 it can be noticed that the pendulum swings more and faster than in the case $(H^*, J) = (0, 0.435)$. And while the behaviours of $x_1(t)$ and $x_2(t)$ are very irregular in Figure 9, in Figure 13 they are somewhat regular. Only the amplitude of the functions change, but the overall shape stays the same. It is also the case here that $x_3(t)$ attains its maximum at approximately 0.8. So in this case the pendulum is able to make turnovers on the 2-sphere. It does not make it to $x_3 = 1$ however, which is due to the presence of the rotation around the x_3-axis. This also leaves a trail of a circle behind at $x_3 \approx 0.8$.

7.4 Pinched Torus

One of the other stationary solutions is the point $(x, y) = (0, 0, 1, 0, 0, 0)$. It is deduced in section 7.1 that this point corresponds with the point $(H^*, J) = (1, 0)$ in the (H^*, J)-plane. However, this point is very unstable. So it is interesting to determine the behaviour of the pendulum in the neighbourhood of this point. Here the counter-image is a ***pinched torus***, which is a torus that is pinched in the point that corresponds to the stationary solution $(x, y) = (0, 0, 1, 0, 0, 0)$.
The flow on this torus then determines the behaviour of the pendulum in the phase space. The movement of the pendulum complementary to this point is an infinitely long trip from the top around the sphere to the top again in the configuration space. This is not easily depicted, but various points close to $(H^*, J) = (1, 0)$ will be investigated in order to find out what is going on at this weird point. Furthermore it will be described what the corresponding solutions will do and it will be pointed out what the differences are between the behaviour of the solutions corresponding to these points.

Point $(H^*, J) = (0.99, 0)$

First the point $(H^*, J) = (0.99, 0)$ is investigated.
Let $x_{i,0}$ and $y_{i,0}$ be denoted by the i-th component of x respectively y, that is the initial value at time $t = 0$.
We have to find initial values for x and y such the next system is satisfied,

$$\begin{aligned} \frac{1}{2}(y_1^2 + y_2^2 + y_3^2) + x_3 &= 0.99 \ , \\ x_1 y_2 - x_2 y_1 &= 0 \ , \\ x_1^2 + x_2^2 + x_3^2 &= 1 \ , \\ x_1 y_1 + x_2 y_2 + x_3 y_3 &= 0 \ . \end{aligned}$$

First we set $x_{3,0} = 0.98$. This value is chosen such that the initial values $y_{1,0}$, $y_{2,0}$ and $y_{3,0}$ do not have to be all equal to zero, which would be silly. Second we set $x_{1,0} = x_{2,0}$ and $y_{1,0} = y_{2,0}$ in order to satisfy the second equation immediately. From the third equation it then follows that $x_{1,0} = x_{2,0} = \sqrt{(1 - (0.98)^2)/2} \approx 0.141$.
Substituting this in the third equation gives

$$\begin{aligned} 2x_{1,0} y_{1,0} + x_{3,0} y_{3,0} &= 0 \ , \\ y_{3,0} &\approx -0.287 y_{1,0} \ . \end{aligned} \tag{12}$$

Then substituting this result in the first equation gives

$$\begin{aligned} y_{1,0}^2 + \frac{1}{2} y_{3,0}^2 + x_{3,0} - 0.99 &= 0 \ , \\ y_{1,0}^2 + 0.041 y_{1,0} - 0.01 &= 0 \ , \\ y_{1,0} = \frac{1}{2}(0.041 \pm \sqrt{0.0417}) &\approx 0.0815 = y_{2,0} \ . \end{aligned}$$

Substituting the value $y_{1,0} \approx 0.0815$ in (12) then gives $y_{3,0} = -0.287 \times 0.0815 \approx -0.0234$.
In Mathematica all six initial values were substituted. Subsequently, Figure 14, which displays the parametric plot of $x_1(t), x_2(t), x_3(t)$ against each other, and Figure 15, which displays the time series of functions $x_1(t), x_2(t), x_3(t)$ against the time t, were found. It is to be noted that the graphs of $x_1(t)$ and $x_2(t)$ are exactly the same, because the initial values were chosen in such a way, that is $x_{1,0} = x_{2,0}$, that the roles of x_1 and x_2 were identical $\forall t \in \mathbb{R}$.

Point $(H^*, J) = (1.01, 0)$

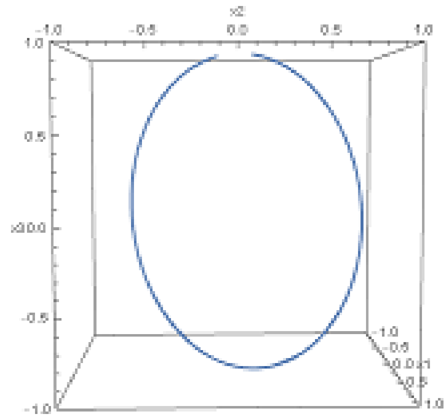

Figure 14: Parametric plot of $x_1(t)$, $x_2(t)$ and $x_3(t)$ for $(H^*, J) = (0.99, 0)$

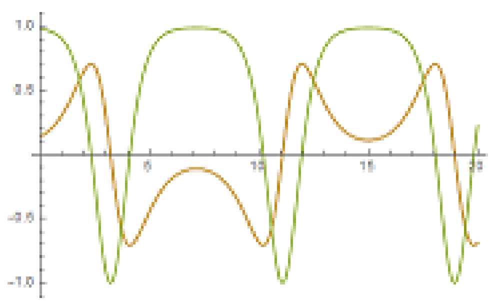

Figure 15: Time series plot of $x_1(t)$, $x_2(t)$ (beige) and $x_3(t)$ (green) for $(H^*, J) = (0.99, 0)$ against the time t

For the point $(H^*, J) = (1.01, 0)$ the same trial and error strategy was applied as in the case $(H^*, J) = (0.99, 0)$, but now with $x_{3,0} = 0.99$. Ultimately this gives

$$\begin{aligned} x_{1,0} = x_{2,0} &\approx 0.0997 \ , \\ x_{3,0} &= 0.99 \ , \\ y_{1,0} = y_{2,0} &\approx 0.132 \ , \\ y_{3,0} &\approx -0.0265 \ . \end{aligned}$$

These six initial value were substituted again in Mathematica and Figures 16 and 17 were the results. Again, Figure 16 displays the parametric plot of $x_1(t), x_2(t), x_3(t)$ against each other, and Figure 17 displays the time series of functions $x_1(t), x_2(t), x_3(t)$ against the time t.

Figure 14 shows that the pendulum falls from a point close to $(0, 0, 1)$ down to $(0, 0, -1)$ and then goes all the way up again to the neighbourhood of $(0, 0, 1)$, but never reaches this point after which is falls down again. This is illustrated by the gap at the top.
In contrast, this gap is closed in Figure 16, which shows that the pendulum will make it to the top and go further at the other side, making endless 2π trips around the sphere.
This contrast is also clarified by the time series plots of both $(0.99, 0)$ and $(1.01, 0)$. Whereas in Figure 15 the graphs of both $x_1(t)$ and $x_2(t)$ do not come above the t-axis when $x_3(t)$ goes to 1 around $t = 5$, the graphs in Figure 17 do.

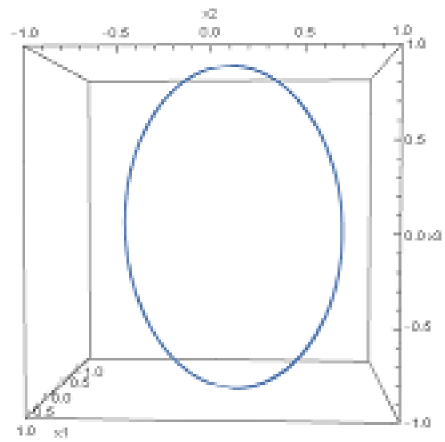

Figure 16: Parametric plot of $x_1(t)$, $x_2(t)$ and $x_3(t)$ for $(H^*, J) = (1.01, 0)$

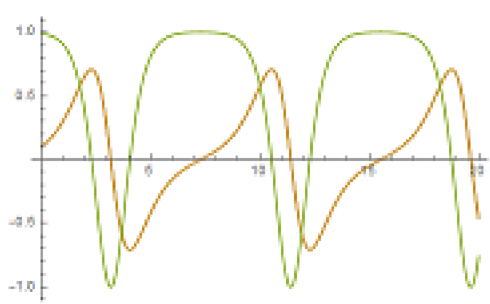

Figure 17: Time series plot of $x_1(t)$, $x_2(t)$ (beige) and $x_3(t)$ (green) for $(H^*, J) = (1.01, 0)$ against the time t

In an attempt to display a more general trajectory rather than only circles (with or without a gap), the points $(H^*, J) = (0.99, 0.01)$ and $(H^*, J) = (1.01, -0.01)$ are investigated also. This is done by the same approach as in the previous subsection. Equation (11) is thus used also.

Point $(H^*, J) = (0.99, 0.01)$

For the point $(H^*, J) = (0.99, 0.01)$ the value $z = 3.91506$ was the result and with the choices $y_3 = 0.5$ and $y_1 = 1$ the next approximations for the initial values were found,

$$\begin{aligned} x_1 &= 0.136448 \ , \\ x_2 &= 0.212751 \ , \\ x_3 &= -0.96753 \ , \\ y_1 &= 1 \ , \\ y_2 &= 1.6325 \ , \\ y_3 &= 0.5 \ . \end{aligned}$$

Putting these approximations in Mathematica and plotting the solutions results in figures 18 and 19.

Point $(H^*, J) = (1.01, -0.01)$

For the point $(H^*, J) = (1.01, -0.01)$ the approach gave $z = 3.95574$ as a result and the next approximations for the initial values were found,

$$\begin{aligned} x_1 &= 0.126152 \ , \\ x_2 &= 0.217509 \ , \\ x_3 &= -0.96787 \ , \\ y_1 &= 1 \ , \\ y_2 &= 1.64491 \ , \\ y_3 &= 0.5 \ . \end{aligned}$$

Putting these approximations in Mathematica and plotting the solutions results in figures 20 and 21.

Figure 18 shows that the pendulum falls from a point close to $(0, 0, 1)$ down to $(0, 0, -1)$ and then goes all the way up again to the neighbourhood of $(0, 0, 1)$ but never reaches this point after which it falls down in another direction. This is illustrated by the gap at the top.
In contrast, this gap is closed in Figure 20, which shows that the pendulum will make it to the top and swing further at the other side.
The behaviour is thus similar to the behaviour in Figures 14 and 16, but now the pendulum falls back or swings further in another direction. There is also a contrast between the time series plots of both $(0.99, 0.01)$ and $(1.01, -0.01)$ and the time series plots of $(0.99, 0)$ and $(1.01, 0)$, but these are not very instructive, as they are very irregular.

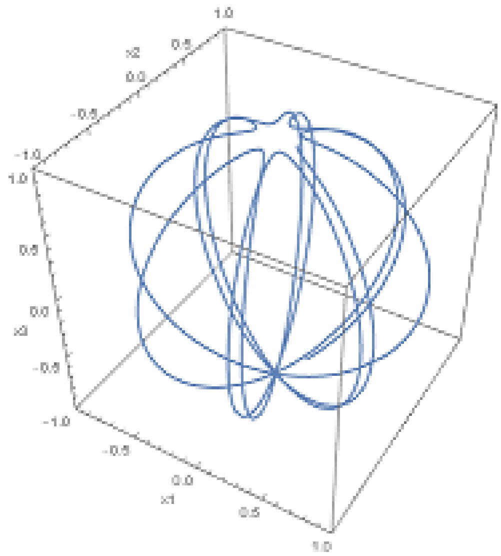

Figure 18: Parametric plot of $x_1(t)$, $x_2(t)$ and $x_3(t)$ for $(H^*, J) = (0.99, 0.01)$

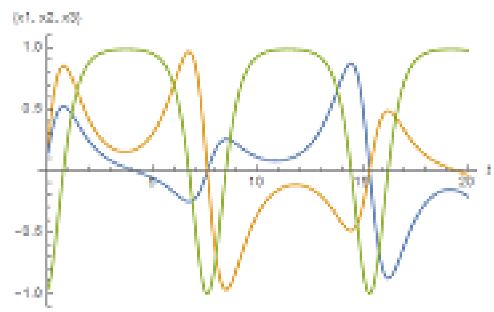

Figure 19: Time series plot of $x_1(t)$ (blue), $x_2(t)$ (beige) and $x_3(t)$ (green) for $(H^*, J) = (0.99, 0.01)$ against the time t

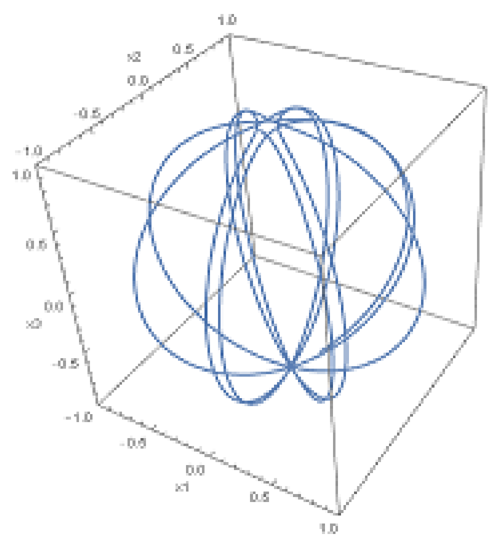

Figure 20: Parametric plot of $x_1(t)$, $x_2(t)$ and $x_3(t)$ for $(H^*, J) = (1.01, -0.01)$

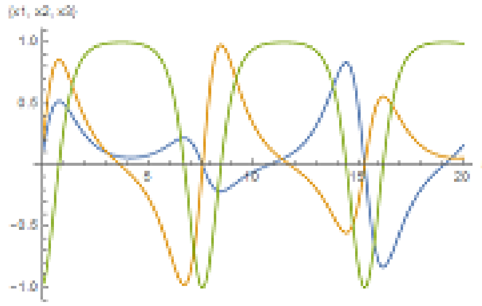

Figure 21: Time series plot of $x_1(t)$ (blue), $x_2(t)$ (beige) and $x_3(t)$ (green) for $(H^*, J) = (1.01, -0.01)$ against the time t

8 Conclusion

In this project we learned about Hamiltonian systems and their solutions in regard of the spherical pendulum. These solutions were found with the help of the Energy momentum mapping. The flow on the counter-images of its critical values (H^*, J) described the periodic solutions and the stationary solutions of the spherical pendulum. Inside the area enclosed by the critical values, the counter-images were described by tori. This is a result of Liouville's Integrability Theorem. The flow on these tori then determined the simultaneous swinging and rotating of the pendulum in the configuration space. Lastly there has been taken a look in the neighbourhood of the weird point $(H^*, J) = (1, 0)$. It turned out that this point marks the difference between turnovers $(H > 1)$ and fall-backs $(H < 1)$ of the pendulum. In this way we have seen 4 different types of solutions.
Further research can expand on the role of the flow of Hamiltonian vector fields in this process. This was mentioned several times, but not deep enough. Moreover, the theory of chaos can step in when the pendulum reaches heights it never reached before.

References

[1] Rowan Lonsdale, A Proof of the Jacobi identity `http://wwwf.imperial.ac.uk/~pavl/Jacobi.pdf`

[2] Cushman, Richard H., Bates, Larry M., Global Aspects of Classical Integrable Systems, Chapter 4: The Spherical Pendulum, 1997, pp. 147-186.

[3] Meiss, James, Hamiltonian Systems, 2007. `http://www.scholarpedia.org/article/Hamiltonian_systems`

[4] Jovanovic, Bozidar, The Teaching of Mathematics, 2011, Vol. 13, pp. 1-14. 'What Are Completely Integrable Hamiltonian Systems.'

[5] B. Sturmfels. Introduction to resultants. In Applications of computational algebraic geometry (San Diego, CA, 1997), volume 53 of Proc. Sympos. Appl. Math., pages 25–39. Amer. Math. Soc., Providence, RI, 1998.